Raytheon

MASS LOADING (TURBIDITY)

VISIBLE/INFRARED IMAGER/RADIOMETER SUITE ALGORITHM THEORETICAL BASIS DOCUMENT

Version 4: May 2001

Alexander P. Vasilkov

Dorlisa Hommel
Kendal Carder, Science Team Member
University of South Florida

RAYTHEON SYSTEMS COMPANY
Information Technology and Scientific Services
4400 Forbes Boulevard
Lanham, MD 20706

SRBS Document #: Y2410

EDR: Mass Loading (Turbidity) (40.7.11)

Doc No: Y2410
Version: 4
Revision: 0

	FUNCTION	NAME	SIGNATURE	DATE
Prepared By	EDR Developer	A. VASILKOV		4/17/00
Approved By	Relevant Lead	D. HOMMEL		
Approved By	Chief Scientist	S. MILLER		
Released By	Algorithm IPT Lead	P. KEALY		

TABLE OF CONTENTS

LIST OF FIGURES

Page

LIST OF TABLES

GLOSSARY OF ACRONYMS AND TERMS

ATBD	Algorithm Theoretical Basis Document
Case 1	Water whose optically active constituents are totally correlated
Case 2	Water whose optically active constituents are totally uncorrelated
CPU	Central Processing Unit
CZCS	Coastal Zone Color Scanner
DOM	Dissolved Organic Matter
EDR	Environmental Data Records
EOS	Edge Of Swath
IOP	Inherent Optical Properties
IORD	Integrated Operational Requirements Document
NIR	Near InfraRed
SeaWiFS	Sea-viewing, Wide Field-of-view Sensor
SPM	Suspended Particulate Matter
SRD	Sensor Requirements Document
SVD	Singular Value Decomposition
SZA	Solar Zenith Angle
TOA	Top Of the Atmosphere
VIIRS	Visible/Infrared Imager/Radiometer Suite

GLOSSARY OF MAIN SYMBOLS

a	The absorption coefficient
$A(\lambda)$	A wavelength-dependent parameter in chlorophyll-specific absorption coefficient parameterization
b_b	The backscattering coefficient
$B(\lambda)$	A wavelength-dependent parameter in chlorophyll-specific absorption coefficient parameterization
C	Chlorophyll concentration
C_i	Concentration of i-th substance
E	Irradiance
f	Averaged value of errors introduced into simulated reflectance spectra
$F(C_i)$	The objective function to be minimized
F_0	Extraterrestrial irradiance
k	The DOM spectral absorption slope
L_w	Water-leaving radiance
m	The sea water refraction index
n	The backscatter spectral ratio exponent
N	A number of wavelengths
Q	The Q-factor
r	The correlation coefficient
$r_{1,2}$	Relative errors of retrieving
R	Diffuse reflectance just below the sea surface
R_{rs}	Remote sensing reflectance
S	SPM concentration
t	Transmittance
w	A random number
X	A ratio of the backscattering coefficient to the sum of the absorption coefficient and the backscattering coefficient
δ	A small perturbation
ε	A parameter characterizing the spectral difference between the chlorophyll-specific and DOM-specific absorption coefficients
$\varphi(\lambda)$	The function characterizing the spectral difference between the chlorophyll-specific and DOM-specific absorption coefficients
λ	Wavelength
θ	Zenith angle
$\sigma(\lambda)$	A weighting function

ABSTRACT

This Mass Loading algorithm is based on minimization of the spectral difference between measured and modeled seawater reflectance or water-leaving radiance. It makes use of visible VIIRS bands. The algorithm provides simultaneous retrievals of chlorophyll concentration, the dissolved organic matter (DOM) absorption coefficient, and the suspended particulate matter (SPM) backscattering coefficient. Mass loading, or, more conventionally, SPM concentration, is determined from the SPM backscattering coefficient using a calibration procedure specific for ocean areas considered. A feature of this algorithm is the possibility of varying the parameters describing the spectral backscatter of SPM and the spectral absorption of DOM when inverting the reflectance model. The parameters are allowed to vary by step increments in the range characteristic for the ocean area concerned. The range of parameter variations is currently set up to cover the whole ocean, from open ocean waters to turbid coastal waters. Regional algorithms can be established by specifying this range. A linear, least squares technique is used to retrieve seawater bio-optical properties from the reflectance model. Hence, the algorithm is computationally fast and may be used for operational purposes.

A sensitivity analysis of the retrievals was carried out for two types of reflectance errors: spectrally uncorrelated random errors (modeling sensor noise), and spectrally correlated errors (modeling atmospheric correction and sensor calibration errors). The analysis showed that chlorophyll concentration was most sensitive to the uncorrelated errors, while SPM backscatter was most sensitive to the correlated errors. End-to-end simulations, which included an atmospheric correction algorithm, showed that the algorithm accuracy for the moderate resolution product met the SRD accuracy requirement of 30 percent with a margin of 5 percent, the algorithm precision was within 25 percent for the entire measurement range. The algorithm uncertainty for the fine resolution product met the SRD uncertainty requirement of 30 percent.

1.0 INTRODUCTION

1.1 PURPOSE

This Algorithm Theoretical Basis Document (ATBD) describes the algorithm used to retrieve mass loading (turbidity) of the Visible/Infrared Imager/Radiometer Suite (VIIRS) Level 2 Product. Mass loading, or suspended particulate matter (SPM) concentration, is measured in mg/l units and retrieved from water-leaving radiances. The document provides the physical theory and mathematical background, includes implementation details, and describes assumptions and limitations of the adopted approach.

1.2 SCOPE

This document covers the algorithm theoretical basis for the retrieval of seawater mass loading from water-leaving radiances. Section 1 describes the purpose and scope of the document. Section 2 provides an overview and background. The algorithm description is presented in Section 3. Section 4 summarizes assumptions and limitations, and references for publications cited in the text are given in Section 5.

1.3 VIIRS DOCUMENTS

References to VIIRS documents are indicated by a number in italicized brackets, e.g., *[V-1]*.

[V-1] Visible/Infrared Imager Radiometer Suite (VIIRS) Payload and Algorithm Development for NPOESS. Vol. II. Technical/Management Approaches. Publication No. 97-0096, 1997.

[V-2] VIIRS Sensor Requirements Document, Technical Requirements Document, 1997.

[V-3] VIIRS Sensor Specification Document, 2000.

1.4 REVISIONS

The original version of this document was dated July 15, 1998. The first revision was dated October 15, 1998. The second version was dated June 1999. The third version was dated May 2000. This is the fourth version of this document, dated May 2001. A minor revision was made to the VIIRS Data section.

2.0 EXPERIMENT OVERVIEW

2.1 OBJECTIVES OF MASS LOADING (TURBIDITY) RETRIEVALS

Mass loading is defined as the concentration of suspended matter in a vertical column in the ocean. This quantity is referred to as "turbidity" in the Integrated Operational Requirements Document (IORD) because it is used to derive both rates of sediment deposition and optical clarity. The term "suspended particulate matter (SPM) concentration" will be used as a synonym to the "mass loading " term throughout the document. The depth of the vertical column is specified by the vertical cell size. We recommend that the vertical cell size threshold should be a function of turbidity because the vertical distance sampled by VIIRS can significantly vary with variations in turbidity.

With respect to remote sensing, two main types of seawater have been defined (Morel and Prieur, 1977; Gordon and Morel, 1983). Case 1 waters are characterized by a strong correlation between scattering and absorbing substance concentrations. The open ocean surface water is typical Case 1 water. The correlation is strong because all the substances originate in biological processes. A primary source of the substances is marine phytoplankton. The majority of light scattering particles in Case 1 waters are detritus and bacteria. Detritus is also the product of phytoplankton degradation. Bacteria feed on products of phytoplankton degradation; therefore, their concentration relates to phytoplankton concentration. Case 1 water can be referred to as one-parameter water, i.e., its optical properties can be described by a single parameter—chlorophyll concentration. Therefore, mass loading of Case 1 water may be derived from chlorophyll concentration. Mass loading of Case 1 waters mainly characterizes the content of phytoplankton, its particulate degradation products, and bacteria in seawater.

Case 2 waters are characterized by a lack of any correlation between scattering and absorbing substance concentrations. Coastal waters are often referred to as Case 2 waters. Marine phytoplankton is not a dominant component of optically active water constituents. Particulate matter arises from river water inflow, bottom resuspension, or coastline erosion. Its concentration does not vary with phytoplankton concentration. For example, tidal resuspension of sediment affects only the suspended sediment concentration and does not immediately affect the phytoplankton pigment concentration. In Case 2 waters the colored dissolved organic matter (DOM) is mainly provided by river inflow. Case 2 water can be referred to as multiparameter water, i. e., its optical properties are described by a set of parameters. Mass loading of Case 2 waters cannot be derived simply from the chlorophyll concentration. A specific algorithm to retrieve SPM concentration from water-leaving radiances is needed. Mass loading of Case 2 waters characterizes content of terrigenic particulate matter in sea water rather than content of phytoplankton, its particulate degradation products, and bacteria. Clarity of Case 2 water is mainly determined by its mass loading. The above classification concept is somewhat idealized because, in reality, all waters belong to an intermediate case.

2.2 INSTRUMENT CHARACTERISTICS

The retrieval of ocean EDRs is based on bio-optical algorithms using spectral reflectance of the sea water column in the visible spectral region. VIIRS has five spectral bands in the visible region *[V-1]*. Their centers are located at wavelengths 412, 445, 488, 555, and 672 nm.

Bandwidths are equal to 18 nm for first two bands and 20 nm for other bands. These bands are traceable to the SeaWiFS and MODIS heritage. The bio-optical algorithms retrieve the Ocean Color/Chlorophyll EDR from remote sensing reflectance of seawater, R_{rs}, which is the output of atmospheric correction algorithms. The atmospheric correction algorithms essentially make use of near infrared (NIR) bands. VIIRS has two NIR bands. They are located at wavelengths 751 and 865 nm. Their bandwidths are 15 and 39 nm respectively. In contrary to SeaWiFS, the first VIIRS NIR band was shifted and narrowed to avoid oxygen absorption at 762 nm. The SeaWiFS NIR band at 765 nm includes the 762 nm oxygen absorption band. Possible interaction between oxygen absorption and scattering of thin cirrus clouds significantly deteriorates the performance of the SeaWiFS atmospheric correction.

.

2.3 RETRIEVAL STRATEGY

Mass loading retrievals will be performed only under clear-sky daytime conditions for regions of the sea surface that have no ice cover. If a cloud mask and an ice cover mask are not applied for a given pixel, the atmospheric correction of top-of-atmosphere radiance is performed. An output of the atmospheric correction algorithm is remote sensing reflectance, which is an input of the mass loading algorithm. Ancillary data sets are needed for the atmospheric correction algorithm only. Mass loading retrievals will be performed provided the values of the water-leaving reflectance are positive in all VIIRS visible bands. The output of the mass loading algorithm is the SPM backscattering coefficient—the inherent characteristic of mass loading. It should be converted to mass loading using either empirical relationships specific to the ocean region considered or relationships proposed in this document for Case 1 and Case 2 waters.

3.0 ALGORITHM DESCRIPTION

3.1 OVERVIEW AND BACKGROUND

All algorithms for retrieval of seawater constituents from spectral reflectance (or water color spectrum) can be divided into two groups: empirical algorithms and analytical algorithms. Empirical algorithms are based on the empirical correlation between reflectance or radiance band ratios and water constituent concentrations. The radiance band-ratio methods for determining the phytoplankton pigment concentration have already been proven useful in global mapping of the ocean phytoplankton pigments (Gordon *et al*., 1983).

Empirical algorithms that retrieve SPM concentration make use of two basic approaches. The first approach is the band-ratio method, which is mostly used for Case 1 waters, where chlorophyll and other optically active substances are highly correlated and chlorophyll concentration is therefore the only parameter determining sea water color. In the second approach, sea water reflectance values in the yellow-red spectral region are correlated to SPM concentration. The physics of the first approach is simple. SPM in Case 1 waters originates from biological processes, and one can expect that a strong correlation between SPM and phytoplankton biomass that is measured in phytoplankton pigment units. Phytoplankton pigment concentration is expressed through radiance band ratios. Therefore, SPM concentration can be related to radiance band ratios as well.

An example of the first approach is the algorithm suggested for (CZCS) spectral bands in the form of:

$$\log S = \log A - B \log \frac{L_w(\lambda_1)}{L_w(\lambda_2)} \tag{1}$$

where S is the SPM concentration (mg/l), $L_w(\lambda_i)$ is the water-leaving radiance for ith band, and A and B are the regression coefficients. For λ_1=440 nm and λ_2=550 nm, regression coefficients are A=0.40 mg/l, and B=0.88 (Clark *et al*., 1980).

Several empirical algorithms were proposed to retrieve the suspended sediment concentration in Case 2 waters. They mostly use the second approach, correlating the SPM concentration to water-leaving radiances. A review of these algorithms was published in Curran and Novo (1988). Various algorithms using the second approach have been developed based on the North Sea optical data collected in coastal waters (Althuis *et al*., 1996). For example, the most appropriate multiple band algorithm makes use of two bands (coefficient of determination r^2=0.81):

$$S(mg/l) = 2.39 - 1.47R(555) + 10.0R(670) \tag{2}$$

where R is the diffuse reflectance.

The so-called semi-empirical algorithms comprise a subgroup of empirical algorithms. They use an ocean color model and empirical regressions between water constituents to gain statistical relationships between sea water constituents and some variables formed from spectral reflectance values. A typical example of this method is described in Tassan (1994). Using a three-component

water color model (Sathyendranath *et al*., 1989), it was found that the optimal algorithm could be written in the form:

$$\log S = 1.82 + 1.23 \log[(R_5 + R_6)(R_1 / R_3)^{-12}] \qquad 0.56 \le S(g/m^3) \le 4.6 \tag{3}$$

where R_i is the reflectance of the *i*-th SeaWiFS band.

These simple empirical algorithms are not reliable for Case 2 coastal waters. In such cases the second group, the so-called analytical algorithms, may be promising. Analytical algorithms minimize the spectral difference between the measured and modeled reflectance spectra:

$$F(C_j) = \frac{\sum_i \left[R_{i\,measured} - R_i(C_j) \right]^2}{\sigma_i^2} \tag{4}$$

where $F(C_j)$ is the objective function, $R_i=R(\lambda_i)$ is the modeled spectral reflectance, C_j is the water constituent concentrations, and $\sigma_i=\sigma(\lambda_i)$ is the spectral weighting function. A general scheme of analytical algorithms is shown in Figure 1.

Analytical algorithms use a reflectance model as well as a model of the spectral Inherent Optical Properties (IOP). The IOPs of water constituents are derived from inversion of the reflectance model, i.e., from minimizing the spectral difference between the modeled reflectance and the *in situ* measured reflectance. The analytical algorithms make use of the spectral models of the IOP. They can be adjusted to local area conditions by specifying parameters describing the spectral dependence of the IOP. Precise values of the parameters should be established from field measurements. There have been many examples of the application of the analytical algorithms to the retrieval of water optical properties and constituent concentrations since 1985 (Burenkov *et al*., 1995; Sugihara *et al*., 1985; Carder *et al*., 1991; Vasilkov *et al*., 1992; Lee *et al*., 1994; Doerffer and Fischer, 1994; Roesler and Perry, 1995; Hoge and Lyon, 1996; Vasilkov, 1997; Garver and Siegel, 1997).

The problem (Equation 4) is nonlinear function minimization. The nonlinear function minimization was used in Burenkov *et al*. (1985); Carder *et al*. (1991); Lee *et al*. (1994); Doerffer and Fischer (1994); Roesler and Perry (1995); and Garver and Siegel (1997). The minimization of a nonlinear function of several variables may be computationally expensive and, therefore, not feasible for operational purposes. An alternative approach is based on a matrix-inversion technique. The radiance model is transformed into a linear equation set with unknowns related to water constituent concentrations. An exact matrix inversion of a seawater radiance model was recently proposed in Hoge and Lyon (1996). The least-squares technique to solve an over-determined system of linear equations was used in Sugihara *et al*. (1985); Vasilkov *et al*. (1992); and Vasilkov (1997). This approach requires less CPU time than the nonlinear function minimization. The algorithm described in this document is based on the least-squares technique applied for solving an over-determined system of linear equations resulting from a seawater reflectance model.

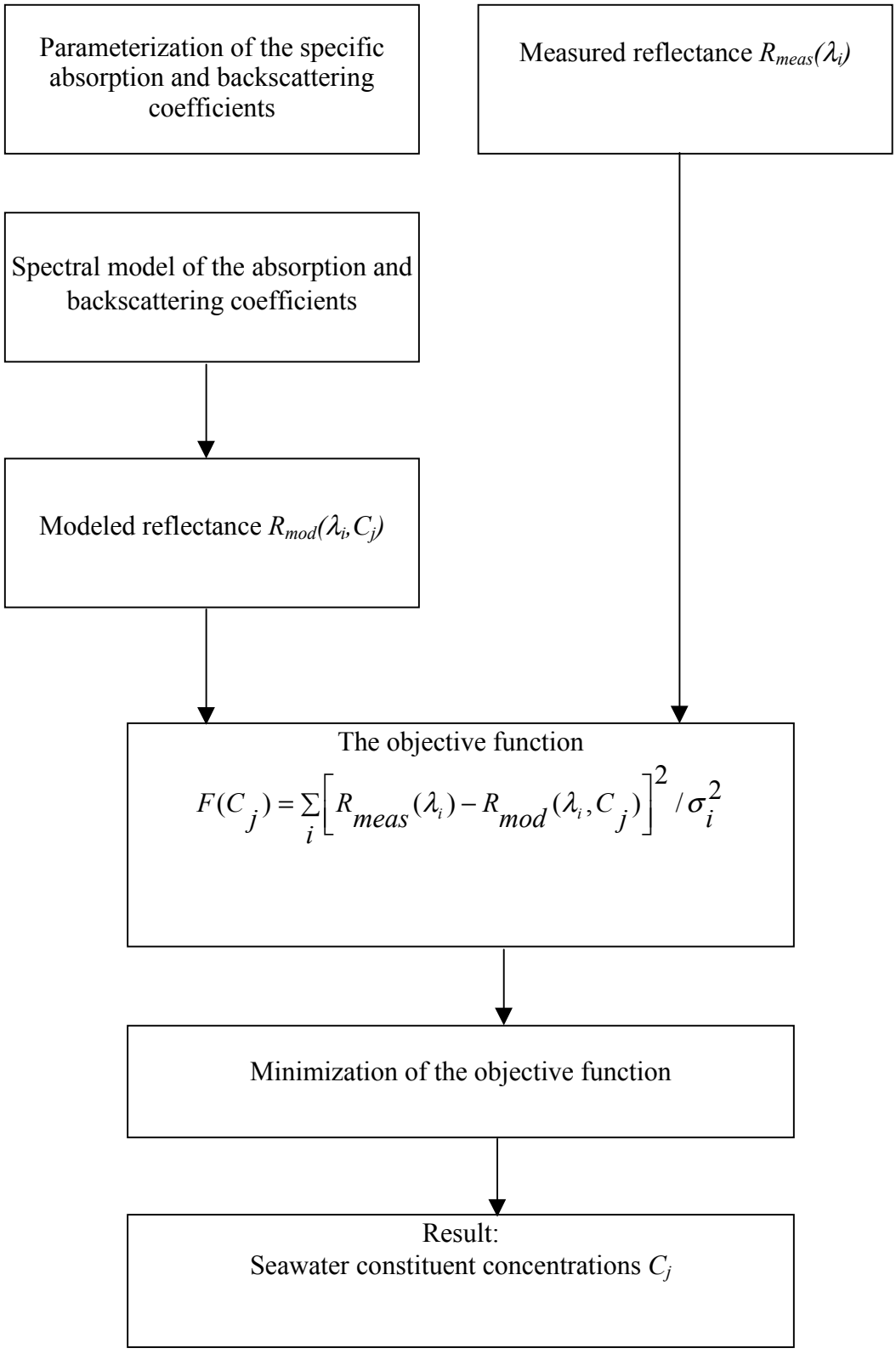

Figure 1. Analytical algorithm flowchart showing that seawater constituents are retrieved from minimization of the spectral difference between the measured and modeled reflectance.

The nonlinear minimization problem (Equation 4) was solved using the Levenberg-Marquardt method (Roesler and Perry, 1995). The total particulate backscatter was partitioned into contributions by large particles with no spectral dependence and by smaller particles with a power law spectral dependence. This involves two backscatter unknowns: b_{01} and b_0. A high correlation between the retrieved backscattering coefficient and the measured total geometric cross-sectional area of particles with equivalent spherical diameters of 2 to 200 μm was reported (r=0.99).

The Levenberg-Marquardt method was also used in Garver and Siegel (1997) for inversion of ocean color spectra measured in the Sargasso Sea. The retrieved chlorophyll estimates showed excellent correspondence to chlorophyll determinations. However, the backscattering coefficient for particles was nearly constant in time and showed no correspondence with the temporal signal observed for chlorophyll concentrations.

An analytical algorithm for retrieval of chlorophyll, suspended matter, and gelbstoff in Case 2 waters was developed in Doerffer and Fischer (1994) to analyze CZCS data. The algorithm will retrieve not only the water bio-optical parameters, but also the aerosol path radiance. This implies that a separate atmospheric correction is not necessary. The algorithm minimizes the spectral difference between the CZCS-measured and modeled radiances. The optimization procedure used in the search loop is the simplex algorithm minimizing the χ^2 statistic of the modeled and CZCS-derived radiances. Satellite-derived data were compared to shipborne measurement data gathered in the German Bight. Good agreement between mean values of retrieved and measured SPM concentration was found.

The least-squares technique was first used in Sugihara *et al*. (1985) to retrieve bio-optical parameters from hyperspectral reflectance data sets gathered in Japanese coastal waters. Correlation between the retrieved SPM backscattering coefficient and measured SPM concentration was rather high, with the correlation coefficient r=0.79. It was shown that the choice of spectral bands could seriously affect the correlation between observed and retrieved concentrations. For example, the use of only four wavelengths (400, 450, 500, and 550 nm) can result in significantly lower correlation.

The least-squares technique also was used in Vasilkov *et al*. (1992) and Vasilkov (1997). A feature of this algorithm is the possibility of varying the parameters describing the spectral backscatter of SPM and the spectral absorption of dissolved organic matter (DOM) when inverting the reflectance model. The parameters are allowed to vary by step increments in the range characteristic for the ocean area concerned. The algorithm adjusted for SeaWiFS visible spectral bands was applied to the spectral reflectance data sets collected in the North Sea coastal waters (Althuis *et al.*, 1996a). The reflectance was measured by a multispectral radiometer placed above the water surface that acquired the spectrum in the range 380-780 nm simultaneously. To correct data for sun/sky glint, the reflectance measured at 752 nm was subtracted from each reflectance spectrum (Althuis *et al*., 1996b). This procedure could not totally exclude the sun/sky contamination of reflectance spectra. Correlation between the retrieved SPM backscattering coefficient and measured SPM concentration was found to be rather high with the correlation coefficient of 0.83.

A crucial question arising in applications of the analytical algorithms is how large errors of retrieval are expected to be for specific areas. The question is commonly answered by a comparison of retrieved results to *in situ* data. The *in situ* data sets are commonly restrictive. Therefore, it is useful to use simulated reflectance data sets to evaluate algorithm errors. Such a sensitivity study was conducted for the exact matrix inversion technique in Hoge and Lyon (1996) and for the least-squares technique in Vasilkov (1997).

The algorithm described in this document is based on a least-squares technique being used to solve an over-determined system of linear equations (Vasilkov *et al*., 1992; Vasilkov, 1997).

3.2 ALGORITHM INPUT

3.2.1 VIIRS Data

Remote sensing reflectances in all VIIRS visible bands (412, 445, 488, 555, and 672 nm) are required as inputs for the mass loading retrieval algorithm. The remote sensing reflectances are the outputs of an atmospheric correction algorithm. Because the visible bands are being used as input to this EDR the same masks and flags are used which are used for the ocean color data. Please see the Ocean Color ATBD for descriptions of the masks and flags used to produce the Mass Loading EDR.

3.2.2 Non-VIIRS Data

The mass loading algorithm does not require non-VIIRS data. Non-VIIRS data sets are only needed for an atmospheric correction algorithm. They include total ozone amount, atmospheric pressure, and surface wind velocity.

3.3 THEORETICAL DESCRIPTION OF MASS LOADING RETRIEVALS

3.3.1 Radiance and Optical Property Models

Many approaches exist to obtain an approximate solution to the radiative transfer equation, which can serve as the marine reflectance model (Gordon, 1973; Golubitskiy and Levin, 1980; Aas, 1987; Haltrin and Kattawar, 1993; Zaneveld, 1982, 1995). They are based on two main physical properties of seawater: first, scattering is highly anisotropic in the forward direction; and second, sea water is an absorbing medium. They ascribe roughly similar dependences of the reflectance on the IOPs: the total absorption coefficient, a; and the total backscattering coefficient, b_b. This dependence can be expressed in a general form $R=f(X)$, where R is the diffuse reflectance, i.e., $R=E_u/E_d$, where E_u and E_d are upwelling and downwelling irradiance just beneath the sea surface, and:

$$X = b_b / (a + b_b) \tag{5}$$

The reflectance is not the seawater IOP and depends, therefore, on conditions of the sea surface illumination. Let the reflectance be expressed as a sum of the diffuse reflectance for direct sunlight illumination and for diffuse skylight illumination (Vasilkov and Stephantsev, 1987):

$$R(\theta_0,\lambda) = gR_{dir}(\theta_0,\lambda) + (1-g)R_{dif}(\lambda) \quad (6)$$

where $g(\theta_0,\lambda)$ is the portion of the direct irradiance in the total irradiance and θ_0 is the solar zenith angle (SZA). It has been shown that R_{dir} depends rather strongly on the SZA (Kirk, 1984; Gordon, 1989; Haltrin, 1997). However, the total reflectance in the 400-700 nm region changes within 10-15 percent over the entire range of the SZA (Vasilkov and Stephantsev, 1987). The change is small because the increase of the reflectance for direct sunlight illumination with SZA increasing is compensated for by reduction of the portion of the direct irradiance in the total irradiance.

A least-squares technique to retrieve the IOP from the reflectance model was suggested in Vasilkov *et al*. (1992) and Vasilkov (1997). The retrieval algorithm is based on a least-squares solution to an over-determined system of linear equations. To invert the reflectance model by the least-squares technique, the general expression $R=f(X)$ must be analytically solvable with respect to X. Following Hoge and Lyon (1996), the reflectance model of Gordon *et al*. (1988) was chosen. According to this model, the ocean reflectance R can be directly related to X by:

$$R/Q = l_1 X + l_2 X^2 \quad (7)$$

where the so-called Q factor is the ratio of the upwelling irradiance to the upwelling radiance toward zenith, and l_1=0.0949 and l_2=0.0794 are constants. The water-leaving radiance is expressed through the reflectance:

$$L_w(\lambda) = F_0(\lambda)t_\lambda(\theta_0)\cos\theta_0 MR(\lambda)/Q(\lambda) \quad (8)$$

where λ is the wavelength, F_0 is the extraterrestrial solar irradiance, t is the diffuse transmittance of the atmosphere, $M=(1-r_E)(1-r_L)/m^2(1-gR)$, r_E and r_L are the Fresnel reflection coefficients of the sea surface for downward irradiance and upward radiance respectively, m is the index of refraction of sea water, $g\approx0.48$ is fraction of upwelling irradiance internally reflected by the sea surface, and θ_0 is SZA. An approximate value of the quantity M is 0.55. Remote sensing reflectance is the ratio of the water-leaving radiance to irradiance just above the sea surface, i.e. $R_{rs}(\lambda) = MR(\lambda)/Q(\lambda)$. For isotropic upwelling radiance, the Q-factor is equal to π, therefore, the remote sensing reflectance is approximately expressed through the diffuse reflectance as follows: $R_{rs} \approx 0.17\,R$.

The total IOP is the sum of the IOP of the pure sea water and the three major scattering and absorbing water substances:

$$b_b(\lambda) = b_{bw}(\lambda) + b_{bp}(\lambda); \qquad a(\lambda) = a_w(\lambda) + a_{ph}(\lambda) + a_{dom}(\lambda) \quad (9)$$

where subscripts *w, p, ph,* and *dom* denote the pure sea water, the particulate matter, the phytoplankton pigments, and the DOM respectively. The detritus absorption is included in the DOM absorption because its spectral dependence (Carder *et al*., 1991) is approximately identical. The pure seawater IOPs were obtained from Smith and Baker (1981). According to the recent findings of Pope and Fry (1997) and Sogandares and Fry (1997) the pure water absorption

coefficient may be notably below the values of Smith and Baker (1981). For Case 2 waters, this difference in the pure water absorption coefficient plays a less significant role than for Case 1 waters (Morel, 1997).

The particulate matter backscattering coefficient and the DOM absorption coefficient are accepted in the conventional form:

$$b_{bp}(\lambda) = b_0(\lambda_0 / \lambda)^n; \qquad a_{dom}(\lambda) = a_0 \exp[-k(\lambda - \lambda_0)] \tag{10}$$

where n is the backscatter wavelength ratio exponent and k is the DOM spectral slope. The parameters k and n vary in distinct ranges. Although parameter k varies within the narrow range 0.01-0.02 nm^{-1} (Bricaud *et al*., 1981), the parameter n can vary within the wide range 0-4 (Lee *et al*., 1994; Hoge and Lyon, 1996). These parameters are normally set as constants in most analytical algorithms. In contrast to other algorithms, the parameters k and n are allowed to vary when inverting the reflectance model.

The phytoplankton absorption coefficient is expressed through the chlorophyll-specific absorption spectrum:

$$a_{ph}(\lambda) = a_{ph0} a^*_{ph}(\lambda, C_{chl}) \tag{11}$$

Dependence of the chlorophyll-specific absorption spectrum on chlorophyll concentration accounts for an increasing package effect from oligotrophic to eutrophic waters and for a possible effect of changing the pigment composition. Different parameterizations of this dependence have been proposed (Carder *et al*., 1991; Bricaud *et al*., 1995; Lee *et al*., 1996). According to Bricaud *et al*. (1995), the chlorophyll absorption coefficient is expressed as

$$a_{ph}(\lambda) = A(\lambda) C_{chl}^{1-B(\lambda)} \tag{12}$$

where $A(\lambda)$ and $B(\lambda)$ are the wavelength-dependent parameters. Using this parameterization and taking $a_{ph0} = a_{ph}(\lambda_0)$, we obtain:

$$a^*_{ph}(\lambda, C_{chl}) = a_{ph}(\lambda) / a_{ph}(\lambda_0) = A(\lambda) C_{chl}^{B(\lambda_0)-B(\lambda)} / A(\lambda_0) \tag{13}$$

Finally, a three-component model of ocean color similar to that of Sathyendranath *et al*. (1989) is obtained. A main distinction is that the model contains two parameters, k and n, which may vary in predefined ranges.

3.3.2 Inversion Technique

In the case of the chlorophyll-specific absorption coefficient being independent of the chlorophyll concentration, Equation 5, in which the value X is given by the solution $X = f^{-1}(R)$ and, therefore, is expressed through the measured reflectance, can be rewritten as a linear expression with respect to the three unknowns b_0, a_{ph0}, and a_0:

$$a_{ph0}a^*_{ph}(\lambda) + a_0 \exp[-k(\lambda - \lambda_0)] + b_0(\lambda_0 / \lambda)^n V(\lambda) = -a_w(\lambda) - b_w(\lambda)V(\lambda) \quad (14)$$

where $V=1-1/X$ is known. Writing Equation 14 for wavelengths λ_i, i=1,2, …,N, one obtains an over-determined system of linear equations for the unknown IOP: $\mathbf{Ax} = \mathbf{B}$, where $\mathbf{A}$ is the $N \times 3$ matrix, $\mathbf{x}$ is a 3-dimensional vector $\{ b_0, a_{ph0}, a_0\}^T$, and $\mathbf{B}$ is an N-dimensional vector. Parameters k and n are inserted in Equation 14 in a nonlinear manner.

A linear least-squares technique is used to solve the set of equations (Equation 14) for the predefined pair of parameters k and n. The parameters are allowed to vary by step increments in the range determined from available data specific to the coastal area concerned. The set of equations (Equation 14) is solved for each pair of k and n. The pair of parameters providing the minimum standard error of the least-squares inversion together with respective IOP is taken as the final solution. Concentrations of water substances should be determined from the IOPs b_0, a_{ph0}, and a_0, by a calibration procedure specific for a local area.

In the case of the chlorophyll-specific absorption coefficient dependent on the chlorophyll concentration, an iteration technique is used. Initially, the chlorophyll-specific absorption coefficient is calculated for average chlorophyll concentration specific for a local area. Then by solving the system of equations (Equation 14), the new value of the chlorophyll concentration is found, and so on. Setting the initial value of the chlorophyll concentration to its average value quickens iteration convergence. The iteration convergence is normally fast; only a few iteration steps are required. The fast convergence of iterations is explained by the relatively weak dependence of the chlorophyll-specific absorption coefficient on chlorophyll concentration.
The algorithm described above is somewhat different from a general type analytical algorithm that searches for a minimum of the functional (Burenkov *et al*., 1985; Lee *et al*., 1994; Dubovik *et al*., 1994; Roesler and Perry, 1995; Garver and Siegel, 1997; Hoogenboom *et al*., 1997):

$$F(b_0, a_{ph0}, a_0) = \sum_i \left[R_{meas}(\lambda_i) - R\ (\lambda_i, b_0, a_{ph0}, a_0)\right]^2 / \sigma^2(\lambda_i) \quad (15)$$

where $\sigma(\lambda)$ is the weighting function and the subscript *meas* denotes the measured reflectance. If the quadratic term in Equation 7 is neglected, the least-squares algorithm will be equivalent to the algorithm (Equation 15) with the weighting function $\sigma = (a + b_b)^{-1}$. That is, the least-squares algorithm minimizes a spectrally weighted difference between the measured and modeled reflectance, and the weighting function is not known *a priori*. A possible difference in the bio-optical parameters retrieved for the least squares and general-type analytical algorithms is considered below.

Numerical implementation of the general-type analytical algorithms is computationally time-consuming. Therefore, their application for processing satellite images may appear to be restrictive. The least-squares algorithm is computationally much faster and could be recommended for processing satellite images.

Varying the parameters k and n when inverting the radiation model was introduced to ensure a positive solution of the equations (Equation 14). The experience of algorithm tests on field data showed that sometimes a negative solution of the equations was encountered in the case of fixed values of the parameters. Special procedures were also undertaken in general analytical algorithms (Equation 15) to avoid meaningless negative results when searching the minimum (Dubovik, 1994).

3.3.3 Conversion of Backscattering Coefficient to Mass Loading

The particulate backscatter b_{bp} is proportional to the SPM concentration:

$$b_{bp} = S \int Q_p(m_p, \lambda_0, r) f(r) dr \tag{16}$$

where Q_p is the backscattering effectiveness for a particle with radius r and the index of refraction m_p, and $f(r)$ is the particle size distribution function. It can be seen from equation 11 that the coefficient of proportionality between the backscattering coefficient and SPM concentration depends on particle substance type and particle size distribution. The particle substance type and particle size distribution can significantly vary with geographic location and season. However, spatial and temporal changes of particle type and particle size distribution are usually neglected, giving a simple relation $b_0 = b^* S$, where b^* is a constant. The algorithm described in this document retrieves the SPM backscattering coefficient as a characteristic of mass loading. The backscattering coefficient can be converted to mass loading using the locally specific coefficient of proportionality between the backscattering coefficient and SPM concentration. Some recommendations concerning this proportionality coefficient follow.

For Case 1 waters it was found that a simple relationship $b(550)=S$, where $b(550)$ is the SPM total scattering coefficient at wavelength 550 nm, is a good approximation (Gordon and Morel, 1983). Morel (1988) suggested an expression for the SPM backscattering coefficient:

$$b_{bp}(\lambda)=b(550)[0.002+0.02(0.5-0.25\log C)(550/\lambda)] \tag{17}$$

where C is the phytoplankton pigment concentration (chlorophyll a +pheophytin) measured in mg m^{-3}. Therefore, for Case 1 waters we obtain the proportionality coefficient in the form:

$$b^*(550)=0.002+0.02(0.5-0.25\log C) \tag{18}$$

It can be seen from Equation 18 that the proportionality coefficient is about 0.02 for oligotrophic waters with characteristic pigment concentration of $C \approx 10^{-2}$ mg/m^3, and becomes about 0.002 for eutrophic waters, with characteristic pigment concentration of $C \approx 10^2$ mg/m^3.

For Case 2 waters, the value $b^* = 0.015$ m^2 /g used at λ_0 = 550 nm in Tassan (1994) can be recommended. However, the problem of deriving the SPM concentration from the backscattering coefficient does not seem to be solved so far. For example, in their recent paper, Hoge and Lyon (1996) stated, “robust relationships need to be developed for obtaining total constituent matter concentration from the total constituent backscatter coefficient.” The major problem seems to be lack of data on simultaneous measurements of the backscattering coefficient and SPM

concentration. Measurements of the SPM concentration are common in research vessels cruises, however, measurements of the backscattering coefficient are so far rare. For example, Hoge *et al*. (1999) stated, "Although shipboard backscattering instrumentation is becoming more available, the data density is still too sparse to be of any real utility for general application to different water masses. We consider knowledge of total constituent backscattering to be fundamental to NASA's satellite algorithm development programs."

Uncertainty in the coefficient converting the SPM backscattering coefficient to the SPM concentration is the major factor affecting the intrinsic algorithm precision or random error. The random algorithm error should include an uncertainty of the mass loading retrievals, which is due to the natural variability of optically active constituents not accounted for by the algorithm. Finally, the natural variability affects the coefficient, which converts the SPM backscattering coefficient to the mass loading. So far, information on the conversion coefficient variability is very limited because of lack of data on simultaneous measurements of the seawater backscattering coefficient and SPM concentration. Presently, a new instrument has been developed to measure the backscattering coefficient, thus, necessary data can be collected (Maffione and Dana, 1997).

3.3.4. Depth of Retrieval

Mass loading is defined as the concentration of suspended matter in a vertical column in the ocean. The depth of the vertical column is specified by the vertical cell size. In the SRD the vertical cell size threshold is specified as to be determined in meter units.

Mass loading EDR is retrieved from ocean color data, i.e. from spectral water-leaving radiance. The water-leaving radiance is effectively formed in an ocean surface layer by diffuse scattering of solar radiation. The depth of this surface layer depends on the diffuse attenuation coefficients for downwelling and upwelling radiation. A characteristic depth of this surface layer may be estimated as $(2K_d)^{-1}$, where K_d is the diffuse attenuation coefficient for downwelling radiation. The diffuse attenuation coefficient, K_d, depends on inherent optical properties of seawater, and therefore, on seawater turbidity. It may vary by as much as a factor of several tens with spatial and temporal variations in optical properties of seawater. For instance, strong variations in optical properties of coastal waters can be caused by storm events or tidal resuspension. Hence, it can be misleading to specify a single value of vertical cell size threshold for mass loading. The vertical cell size threshold, currently listed as 'surface layer (TBD m)', could be specified as a function of turbidity. This function calculated for the Case 1 water diffuse attenuation model (Morel, 1988) is shown in Figure 2 .

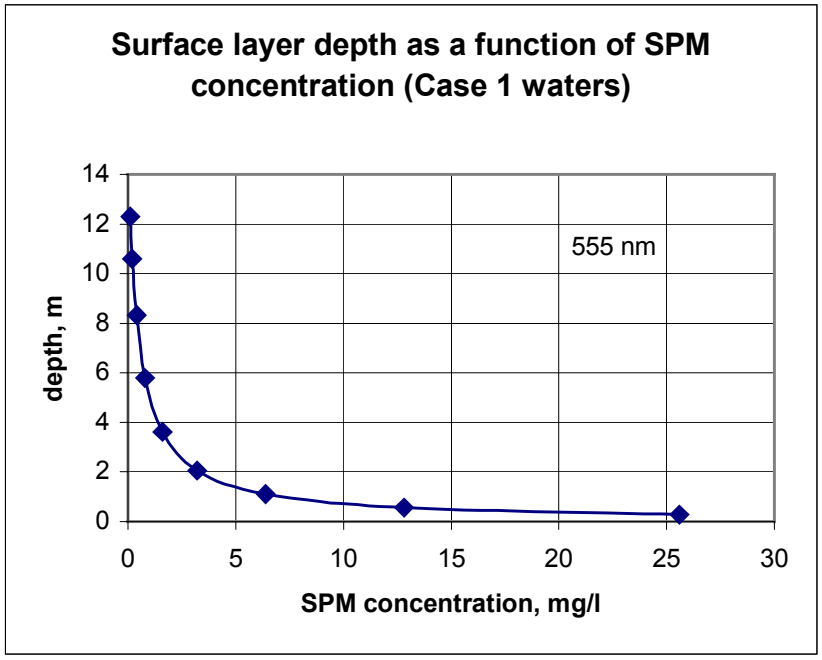

Figure 2. Surface layer depth which effectively forms the backscattered light as a function of SPM concentration.

3.4 ALGORITHM SENSITIVITY STUDIES

3.4.1 General Consideration

There is no common error estimation for analytical algorithms. An accuracy of fitting the measured reflectance with the modeled reflectance cannot serve as the final measure of retrieval errors. The fitting can be excellent, but at the same time a retrieval of bio-optical parameters can be faulty due to an improper model of the spectral reflectance or the IOPs of seawater.

A general approach of small perturbations can be applied for the general-type analytical algorithm (15) to evaluate errors in the retrievals caused by errors in the measured reflectance, or by uncertainties of the IOP-property model (Vasilkov and Kelbalikhanov, 1991). Let the vector that minimizes the function (15) be called $x_j^0=\{b_0, a_{ph0}, a_0\}$, j=1,2,3, and the change in the j-th component of this vector caused by small changes, δR_i, in the measured reflectance for bands i=1,2,...,N be called δx_j. Using a necessary condition of the minimum (15), one can linearly express the perturbations in the retrievals, δx_j, through the perturbation in the measured reflectance, δR_i.

In general, model reflectance can be written as a function $R(x_1 x_1^*, x_2 x_2^* + x_3 x_3^*)$, where x_j^* is the constituent-specific coefficient (assuming that it does not depend on x_j). Let us denote the spectral difference between the chlorophyll-specific and DOM-specific absorption coefficient through a function $\varepsilon\varphi(\lambda)$:

$$x_3^*(\lambda) = Const\ x_2^*(\lambda)[1+\varepsilon\varphi(\lambda)] \qquad (19)$$

In the case of small values of the parameter ε, it can be shown that errors in reflectance are amplified in chlorophyll and DOM retrievals as ε^{-1}. The SPM retrievals are less sensitive to the perturbations.

The error amplification is typical for ill-conditioned problems. A principal physical reason is that the spectral behavior of the DOM and phytoplankton pigment specific-absorption coefficients is similar. They both decrease into the long-wavelength region in the same manner. There is a difference in spectral behavior only in the violet and red spectral regions. However, the red spectral region difference is less valuable in distinguishing the DOM and pigment absorption because of either too low a value of the water-leaving radiance for clear waters or the influence of chlorophyll fluorescence for turbid waters. That is why the 412 nm spectral band added in the new generation of ocean color sensors plays a key role in distinguishing the DOM and pigment absorption.

An example of values of $\varepsilon\varphi(\lambda)$ for the SeaWiFS spectral bands is given in Table 1.

Table 1. Spectral Difference Between Dissolved Organic Matter and Chlorophyll-specific Absorption Coefficient

Wavelength, nm	412	443	490	510	555	670
$\varepsilon\varphi(\lambda)$	0.72	0.0	-0.177	-0.117	0.03	-0.438

The values of $\varepsilon\varphi(\lambda)=\exp[-k(\lambda-443)]-a^*_{ph}(\lambda,C_{chl})/a^*_{ph}(443,C_{chl})$ were calculated for the average DOM spectral slope k=0.014 nm^{-1} (Bricaud *et al*., 1981) and the chlorophyll-specific absorption spectrum for chlorophyll concentration C_{chl} = 1 mg/m^3 (Bricaud *et al*., 1995). The absolute value of $\varepsilon\varphi(\lambda)$ averaged over a spectral range from 410 to 670 nm is of the order of magnitude 10^{-1}.

For the least-squares algorithm, the sensitivity of the retrieval to reflectance errors and/or IOP model uncertainties is determined by properties of the 3×3 matrix $\mathbf{A}^T\mathbf{A}$. It can also be shown that with $\varepsilon<<1$, errors in reflectance are amplified in retrievals as ε^{-1}. The estimate of the retrieval error in the form of ε^{-1} gives only an order of magnitude of the error. To obtain specific values of the error, rather complicated calculations of the inverse matrix should be carried out. Instead of that, a numerical study of the least-squares algorithm sensitivity to reflectance errors was performed.

Another approach to theoretical estimation of retrieval errors was used in Vasilkov *et al*. (1992) and Dubovik *et al*. (1994). The retrieval error was estimated using some statistical assumptions concerning the spectral reflectance and probability distribution of retrieved quantities. The estimation of retrieval errors can also be performed without any assumptions using a numerical simulation of the measured reflectance (Hoge and Lyon, 1996; Vasilkov, 1997). In order to estimate errors, the bio-optical parameters to be retrieved are defined first. A forward problem is solved to calculate the spectral reflectance corresponding to the input parameters. Then the

spectral reflectance is disturbed by an error introduced into a single spectral band of a sensor (Hoge and Lyon, 1996) or by a random error introduced into all the bands (Vasilkov, 1997). The simulated reflectance is inverted to retrieve the bio-optical parameters. The retrieved values of the bio-optical parameters are compared to the values defined initially.

3.4.2. Sensitivity Study on Simulated Reflectance Data Sets

3.4.2.1 Generation of Data Sets

To produce simulated reflectance data sets for the sensitivity study described in Vasilkov (1997), the initial values b_{0}, a_{ph0}, and $a_{0,}$ together with parameters S and $n,$ were accepted. Then the reflectance $R(\lambda_i)$ was calculated for the VIIRS visible bands. Reflectance spectra were also generated for SeaWiFS visible spectral bands with wavelengths λ_i, i=1,...,6 set to 412, 443, 490, 510, 555, and 670 nm.

The exact reflectance was disturbed by random errors introduced into all spectral bands:

$$R_{simul}(\lambda_i) = R_{exact}(\lambda_i)(1 + fw_i) \tag{20}$$

where i=1,...,6, f is the value of relative error, w_i are normally-distributed random numbers with mean equal to zero and standard error equal to unity. These random errors modeled radiometric sensor noise.

The simulated reflectance spectra are inverted to obtain the retrieved values of IOP. The relative standard deviation of the retrieved IOP, that is, the standard deviation divided by the initial value of the IOP, was calculated over results of the inversion for all simulated spectra. A preliminary conclusion of the error sensitivity study by Vasilkov (1997) is that random errors in the spectral reflectance are amplified by the inversion procedure. For example, the backscatter retrieval error is about 40 percent, and the pigment absorption error is about 25 percent for a ±5 percent random error in the spectral reflectance. Setting the parameters k and n to have exact values for inversion results in a considerable improvement in the retrieval accuracy of the sediment backscatter, but only a slight improvement in the retrieval accuracy of the pigment absorption. Backscatter retrieval errors were reduced approximately by a factor of 3.

A more general sensitivity study was performed for both VIIRS and SeaWiFS spectral bands. Generated IOPs modeled bio-optical parameters of both Case 1 and Case 2 waters. To model Case 2 waters, statistical characteristics of measured bio-optical parameters of the North Sea were used. Coastal waters of the North Sea are typical examples of Case 2 waters. They are characterized by low correlation among major optically active substances (the maximum correlation coefficient is less than 0.5) (Althuis *et al*., 1996a). Therefore, values of bio-optical parameters for reflectance modeling can be set independently to generate reflectance data sets.
An analysis of data sets collected according to Althuis *et al*. (1996a) showed that variability of the SPM concentration, the chlorophyll *a* concentration, and the DOM absorption coefficient can be well represented by the log-normal distribution known as a useful model for bio-optical variability (Campbell, 1995). Parameters of the probability density function of the log-normal

distribution were found and used to produce IOP data sets with a Gaussian random number generator. Parameters of the probability density function of the log-normal distribution:

$$p(x) = \frac{1}{\sqrt{2\pi}\sigma x}\exp\left[-\frac{(\ln x - \mu)^2}{2\sigma^2}\right] \tag{21}$$

where μ and σ are the mean and mean-squared deviation of $\ln x$, are given in Table 2.

Table 2. Means and Standard Deviations for the Log-normal Distribution of Measured Bio-optical Parameters

	μ, the mean	σ, the standard deviation
Chlorophyll *a* concentration, mg/m^3	1.63	0.870
SPM concentration, mg/l	1.82	1.08
DOM absorption coefficient at 412 nm, m^{-1}	-1.28	0.423
DOM spectral slope, nm^{-1}	-4.17	0.154

About 5,000 reflectance spectra were generated in every numerical experiment. The chlorophyll absorption and SPM backscattering coefficients were calculated according to the following formulas (Bricaud *et al*., 1995; Gordon and Morel, 1983):

$$a_{ph}(\lambda) = C_{chl}A(\lambda)C_{chl}^{-B(\lambda)}; \qquad b_{bp}(\lambda) = r_p S\,(550/\lambda)^n \tag{22}$$

with r_p=0.015 m^{-1}/(mg/l) (Tassan, 1994) and n=0. The chlorophyll-specific absorption coefficient independent of chlorophyll concentration was also used, i.e., $B(\lambda) \equiv 0$. The DOM spectral slope was set to the mean, k =0.016 nm^{-1}, for all spectra simulated because of its small standard deviation. An example of generated reflectance spectra is shown in Figure 3. Some spectra have unrealistically large values of the reflectance due to low values of DOM and chlorophyll absorption and high values of the SPM backscatter, simultaneously generated by chance. However, similar large values of the spectral reflectance have been reported for very turbid waters of the Rhone river plume (Ouillon *et al*., 1995). It should be noted that the spectra in Figure 3 are of the diffuse reflectance, values of the remote sensing reflectance are substantially lower.

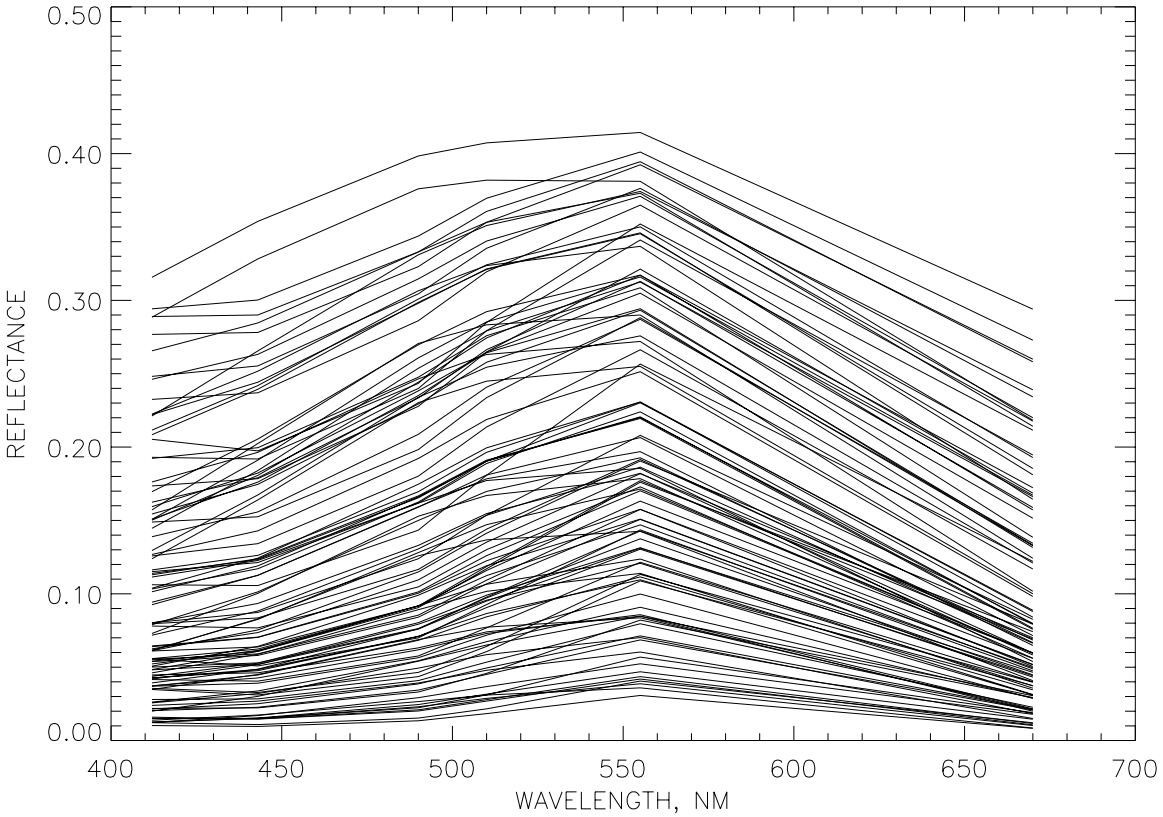

Figure 3. Example of Case 2 water reflectance spectra generated.

To generate Case 1 water reflectance spectra, the Morel reflectance model was used (Morel, 1988). A random number generator with the log-normal distribution was used to produce a chlorophyll concentration data set. The DOM absorption was assumed to be one-fifth of the total absorption of pure seawater and chlorophyll at 440 nm (Bricaud *et al.*, 1981). The SPM concentration was determined according to the relationship $S=b_p(550)$, where b_p is the SPM scattering coefficient (Gordon and Morel, 1983). For Case 1 waters the SPM scattering coefficient is directly related to the chlorophyll concentration through the empirical relationship

$$b_p(550)=0.3C^{0.62}, \tag{23}$$

where C is the chlorophyll concentration in mg/m^3 (Morel, 1988).

The exactly computed reflectance was disturbed by errors introduced into all spectral bands in two ways. First, the reflectance was disturbed by spectrally uncorrelated random errors introduced into all spectral bands according to Equation 20. This spectrally uncorrelated random error emulates radiometric sensor noise. In the second, the reflectance was disturbed by a spectrally correlated error modeling sky radiance reflection that was not completely removed from the measured reflectance, i.e., imperfect atmospheric correction:

$$R_{simul}(\lambda_i) = R_{exact}(\lambda_i)[1 + fw\ (\lambda_i / \lambda_0)^{-\alpha}] \tag{24}$$

where f is the average relative error in a red band (λ_0=672 nm), w is the random number with mean and standard error equal to unity, and α is the Angstrom exponent that characterizes the wavelength dependence of aerosol radiance.

Retrieved values of the bio-optical parameters were compared to the initial values by calculating statistical characteristics: means; the correlation coefficient; relative error of linear regression between the retrieved and initial values; and average relative errors of the retrievals which are calculated as follows:

$$r_1 = \langle \frac{| x_j^{retr} - x_j^{init} |}{x_j^{init}} \rangle, \quad r_2 = \frac{\sqrt{\langle (x_j^{retr} - x_j^{init})^2 \rangle}}{\langle x_j^{init} \rangle} \tag{25}$$

where x_j , j=1,2,3 is the bio-optical parameter, superscripts *retr* and *init* denote the retrieved and initial values respectively, and brackets <...> denote values averaged over all inversions of the simulated reflectance. Both estimations of the retrieval error are close to each other, although the estimation of r_2 is slightly higher. We use the estimation of r_1 in discussion below.
In all cases the reproduction of the simulated reflectance spectra by retrieved reflectance spectra was quite good. A spectrally averaged deviation between the simulated and retrieved reflectance spectra was usually a few percent, reaching 10 percent in rare cases.

3.4.2.2 Atmospheric Correction and/or Sensor Calibration Errors

There are no errors in the algorithm retrievals in the case of undisturbed reflectance. The algorithm exactly retrieves bio-optical parameters if no errors are introduced into the simulated reflectance. This is valid whether the chlorophyll-specific absorption coefficient is dependent on chlorophyll concentration or independent of chlorophyll concentration.

Consider first the results of inverting the simulated reflectance for the chlorophyll-specific absorption coefficient independent of chlorophyll concentration (taken at a fixed value C_{chl}=1 mg/m^3). Some results of retrievals for the case of atmospheric correction errors introduced into VIIRS and SeaWiFS bands are given in Table 3. The average relative error in the red band was taken to be f=20 percent (i.e., reflectance values at 672 nm were, on the average, 20 percent higher than the exact values). In the inversion procedure the parameters k and n were allowed to vary within ranges $0.014 \le k \le 0.018$ nm^{-1}; $0 \le n \le 1$ with increments Δk =0.001 nm^{-1}; Δn =0.1. The range for the spectral slope, k, was taken as the mean plus/minus the standard deviation according to measurement data sets collected in coastal waters of the North Sea (Althuis *et al*., 1996a).

Scatter of retrieved values of the SPM concentration versus initial values is shown in Figure 4. There is systematic overestimation of SPM concentration values in comparison with initial values. This is because the simulated reflectance is always set higher than the exact reflectance while modeling the sky-reflected contribution to the reflectance.

Table 3 shows that relative errors of the mass loading retrievals are rather close for VIIRS and SeaWiFS sensors. Atmospheric correction errors are not amplified in the retrievals. The retrieval errors are the same order of magnitude as errors in the red band reflectance. Increasing the

Angstrom exponent up to unity does not affect the mass loading retrieval errors. Data in Table 3 were obtained with the parameters k and n varying while inverting the reflectance model. If the parameters k and n are set to values used in the reflectance data generation (k=0.016 nm^{-1} and n=0), the relative error of the mass loading retrievals is reduced only weakly.

Table 3. Errors in the Retrievals for Spectrally Correlated Errors in Reflectance

Angstrom Exponent	Bio-Optical Parameter	VIIRS Average Relative Error, R_1, %	SeaWiFS Average Relative Error, R_1, %
0.0	C	10.8	12.2
	a_0	7.1	7.2
	S	28.9	21.0
1.0	C	12.4	15.7
	a_0	12.0	13.3
	S	29.0	21.5

Figure 4. Comparison of initial and retrieved SPM concentrations.

The dependence of the relative error in the retrievals on the average error in the reflectance in the red band is shown in Figure 5. The Angstrom exponent simulating the atmospheric errors in the reflectance was set to unity. Results show that the SPM concentration retrieval is most sensitive to spectrally correlated errors in the reflectance.

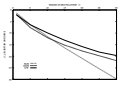

Figure 5. Dependence of the relative error in the retrievals on the average error in the red band reflectance (Angstrom exponent set to unity, the chlorophyll-specific absorption coefficient independent of the chlorophyll concentration).

The dependence of the relative error in the retrievals on the average error in the reflectance in the red band is also shown in Figure 6 for the case of the chlorophyll-specific absorption coefficient dependent on the chlorophyll concentration according to Bricaud *et al*. (1995). A comparison of Figures 5 and 6 shows that setting the chlorophyll-specific absorption coefficient dependent on the chlorophyll concentration mainly results in significant increases (approximately twofold) in the retrieval error in the chlorophyll concentration. The retrieval errors in the DOM absorption coefficient and SPM concentration remain almost the same.

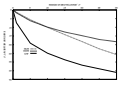

Figure 6. Dependence of the relative error in the retrievals on the average error in the 672 nm reflectance (Angstrom exponent set to unity, the chlorophyll-specific absorption coefficient dependent on the chlorophyll concentration).

A threshold for mass loading precision was established at 30 percent, as was a threshold for mass loading accuracy *[V-2]*. Figures 5 and 6 show that errors in water-leaving radiance in the 672 nm band caused by sensor calibration and/or atmospheric correction errors must be within 20 percent.

3.4.2.3 Radiometric Noise Errors

Consider first the results of inverting the simulated reflectance for the case where the chlorophyll-specific absorption coefficient is independent of chlorophyll concentration (taken at a fixed value C_{chl}=1 mg/m^3). The results of inverting reflectance spectra with random perturbations f=5 percent introduced in all spectral bands are given in Table 4. Scatter of retrieved values of the SPM concentration versus initial values is shown in Figure 7. In the inversion procedure the parameters k and n were allowed to vary within ranges $0.014 \le k \le 0.018$ nm^{-1}; $0 \le n \le 1$ with increments Δk =0.001 nm^{-1}; Δn =0.1. The errors of retrievals are also given in Table 4 for the parameters k and n fixed at the exact values k=0.016 nm^{-1}, n=0.

It can be seen from Table 4 that random perturbation of reflectance spectra leads to relatively great errors in the chlorophyll and DOM retrievals. The chlorophyll concentration and DOM retrieval error is 5-7 times greater than the reflectance error. That means the random error in the reflectance is amplified in the chlorophyll and DOM retrievals. The spectrally uncorrelated random error affects the mass loading retrievals weaker than the chlorophyll and DOM retrievals. The mass loading retrieval error is only twice the average error in the reflectance.

Table 4. Errors in the Retrievals for Spectrally Uncorrelated Random Errors in Reflectance

Range of Parameter *k*	Bio-Optical Parameter	VIIRS Average Relative Error, R_1, %	SeaWiFS Average Relative Error, R_1, %
0.014-0.018 nm-1	C	36.0	33.0
	a	36.2	27.4
	S	10.8	10.1
Fixed 0.016 nm-1	C	33.7	26.3
	a	20.7	17.0
	S	8.7	8.1

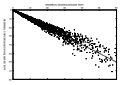

Figure 7. Comparison of the retrieved and initial SPM concentration (5 percent random error in reflectance; the chlorophyll-specific absorption coefficient independent of the chlorophyll concentration; $0.014<k<0.018$ nm^{-1} while inverting).

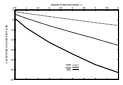

Dependence of the relative error in the retrievals on the error in the reflectance is shown in Figure 8.

Figure 8. Dependence of the relative error in the retrievals on the error in the reflectance (the chlorophyll-specific absorption coefficient independent of the chlorophyll concentration; 0.014<k<0.018 nm^{-1} while inverting).

Consider now the results of inverting the simulated reflectance for the case of the chlorophyll-specific absorption coefficient dependent on chlorophyll concentration. The results of inverting reflectance spectra with random perturbations f=5 percent introduced in all spectral bands are given in Table 4. Scatter of retrieved values of the SPM concentration versus initial values is shown in Figure 9. In the inversion procedure the parameters k and n were allowed to vary within ranges $0.014 \le k \le 0.018$ nm^{-1}; $0 \le n \le 1$ with increments Δk =0.001 nm^{-1}, Δn=0.1. From a comparison of Figure 7and Figure 9, it is seen that the scatter of retrieved SPM concentration points about a regression line $y=x$ is weakly increased for the case of the chlorophyll-specific absorption coefficient dependent on chlorophyll concentration.

Figure 9. Comparison of the retrieved and initial SPM concentration (5 percent random error in reflectance; the chlorophyll-specific absorption coefficient dependent on the chlorophyll concentration; $0.014<k<0.018$ nm^{-1} while inverting).

Some statistical characteristics of the retrievals are given in Table 5 for cases of the parameter k varied and fixed at k=0.016 nm^{-1}.

Table 5. Errors in the Retrievals for Spectrally Uncorrelated Random Errors in the Reflectance

Range of Parameter *k*	Bio-Optical Parameter	VIIRS Average Relative Error, r_1, %	SeaWiFS Average Relative Error, r_1, %
0.014-0.018 nm^{-1}	*C*	75.2	70.8
	a	30.6	20.5
	S	9.8	11.2
Fixed 0.016 nm^{-1}	*C*	63.0	58.6
	a	16.0	13.6
	S	8.4	10.3

A comparison of Tables 4 and 5 shows that the chlorophyll concentration retrieval error is considerably higher for the case of the chlorophyll-specific absorption coefficient dependent on

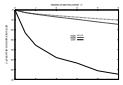

chlorophyll concentration. At the same time the DOM absorption coefficient and SPM concentration retrieval errors are not changed significantly.

Dependence of the relative error in the retrievals on the error in the reflectance is shown in Figure 10. A comparison of this figure with Figure 8 reveals that setting the chlorophyll-specific absorption coefficient dependent on chlorophyll concentration results in considerable enhancement of the chlorophyll concentration retrieval error. The DOM absorption coefficient and SPM concentration retrieval errors do not change significantly.

Figure 10. Dependence of the relative error in the retrievals on the error in the reflectance (the chlorophyll-specific absorption coefficient dependent on the chlorophyll concentration; $0.014<k<0.018$ nm^{-1} while inverting).

A study of the sensitivity of the least squares algorithm to spectrally uncorrelated errors in the reflectance shows that the chlorophyll concentration retrievals are most sensitive to this type of error while the SPM retrievals are less sensitive. Simulations for Case 1 waters showed that the results are quite close to the results obtained for Case 2 waters.

Algorithm sensitivity to VIIRS radiometric noise was also studied using simulated top-of-atmosphere (TOA) radiances. TOA radiances over the ocean were simulated in the VIIRS visible bands using the 6S computer code of Vermote *et al*. (1997). This code uses the Case 1 water reflectance model (Morel, 1988) to simulate water-leaving radiance for a given chlorophyll concentration and performs forward transfer to the top of the atmosphere. The SPM backscattering coefficient is completely determined by chlorophyll concentration according to this seawater reflectance model. The simulations were done for the VIIRS 1330 orbit and standard atmospheric parameters: water vapor content 0.85 g/cm2, ozone content 0.395 cm atm, aerosol type maritime, visibility 23 km, and wind speed 5 m/s. A swath width was assumed to be

2400 km. Chlorophyll concentrations were 0.1, 1.0, and 5 mg/m^3. The corresponding SPM concentrations were 0.072, 0.3, and 0.82 mg/l.

Sensor noise was added to the simulated TOA radiances for each of the seven VIIRS sensor performance models described by Hucks (1998 The sensor model 1 has an effective aperture diameter of 29 cm. Each subsequent sensor model has the effective aperture diameter of 5 cm less. All other sensor parameters are fixed for the sensor models. However, the sensor noise models do not necessarily imply those aperture sizes. Noise equivalent delta radiance (NEdN) was calculated following Hucks (1998) using bandwidths of 20 nm for the VIIRS visible bands. Pixel aggregation was made to obtain the horizontal cell size of 1.3 km.

Retrieval of SPM concentration from TOA radiances was performed in two steps. First to isolate radiometric noise effects on SPM retrievals, the exact atmospheric correction was performed to obtain remote sensing reflectances. The bio-optical algorithm was then used to retrieve SPM concentrations from the remote sensing reflectances. The exact atmospheric correction meant that atmospheric path radiance was simply subtracted from the simulated noise-added TOA radiances. The SPM precision was calculated as the standard deviation of the retrieved values over the whole orbit swath divided by the mean of the SPM concentration. The SPM accuracy was also calculated.

Some results of SPM precision calculations are shown in Figure 11. From Figure 11 it is seen that the precision threshold of 30% is not met for high chlorophyll concentrations. This is explained by low values of the Case 1 water reflectance for high chlorophyll. According to CZSC-derived global chlorophyll statistics (Antoine *et al*., 1996), eutrophic waters with chlorophyll concentration greater than 1 mg/m^3 comprise only 2.4% of the ocean area. The SPM accuracy does not depend on sensor noise level at least for Sensor Models 1 to 5.

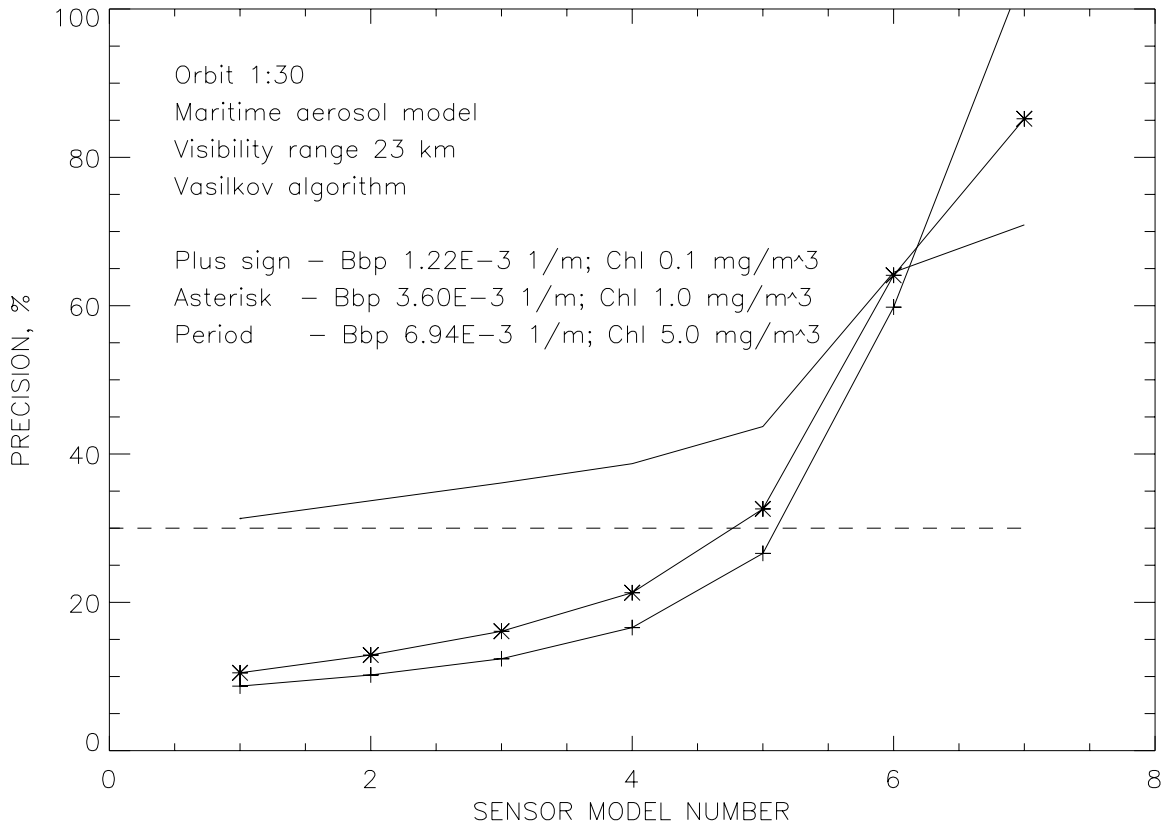

Figure 11. SPM retrieval precision as a function of Sensor Model number.

3.4.2.4 Uncertainty in Pure Sea Water Absorption

For Case 2 waters the effect of uncertainty of the pure sea water absorption coefficient on the retrievals is relatively small because of a small contribution of water absorption to the total absorption. The effect of uncertainty in the pure seawater absorption coefficient on the retrievals was numerically estimated using simulated reflectance spectra. The simulated reflectance spectra were computed using "new" values of the pure seawater absorption coefficient (Pope and Fry, 1997). Inversion of the simulated reflectance spectra was performed using "old" values of the pure sea water absorption coefficient (Smith and Baker, 1981). Retrieved values of the bio-optical parameters were systematically underestimated in comparison to initial values. Systematic underestimation occurs because the pure seawater absorption coefficient uncertainty produces spectrally correlated error in the reflectance. Relative errors in the retrievals were small, and equal to 4.1 percent in the chlorophyll concentration and 2.1 percent in the SPM concentration.

For Case 1 waters "new" values of the pure seawater absorption coefficient dramatically change the spectral reflectance because of the big contribution of pure seawater absorption to total absorption of seawater (Morel, 1996). Therefore, relative errors in the retrievals appear to be considerably greater than for Case 2 water. The relative error of chlorophyll retrievals is about 35 percent and the relative error of SPM retrievals is about 15 percent. This result highlights the

importance of the precise knowledge of pure seawater optical properties for Case 1 waters that comprise most areas of the world's oceans.

3.4.3 Comparing the Least-Squares Technique and the General-Type Analytical Algorithms

A difficulty with the inversion procedure for general-type analytical algorithms is that the function to be minimized is nonlinear. Several iterative methods have been used for solving the problem. A predictor-corrector approach was used in Carder and Steward (1985) and Lee *et al*. (1994). The Levenberg-Marquardt method was used in Roesler and Perry (1995) and in Hoogenboom *et al*. (1997). The Gauss-Newton algorithm was employed in Garver and Siegel (1997). A new iteration-regularization method was proposed in Dubovik *et al*. (1994). A global minimum of the function (Equation 18) may provide unrealistic and even meaningless solutions. Moreover, reaching the minimum of the function (Equation 18) numerically is not easy because the function usually has small gradients in its vicinity over some directions in the three-dimensional space of unknowns. Therefore, additional difficulties with the nonlinear inversion procedure are to ensure the uniqueness of the solution and to avoid unrealistic and even physically meaningless solutions. A simple, reliable method of trials was used in Burenkov *et al*. (1985). It is not computationally effective, but it ensures a unique and realistic solution.

In comparing the least-squares technique to the general analytical algorithms, we used both Newton-type and trial methods. Range constraints of $0<x_j<x_{jmax}$, where x_{jmax}, j=1,2,3 are predefined maximum values of the bio-optical parameters, were imposed while searching the minimum of the function (Equation 15). These constraints prevent meaningless solutions. Both simulated and measured (Althuis *et al*., 1996) reflectance spectra were used in inversion algorithms. Comparison of results for the least squares algorithm and the general analytical algorithm was determined by calculating the correlation coefficients and relative errors according to Equation 24. An example of the comparison is given in Table 6 for simulated reflectance spectra perturbed by uncorrelated random errors.

A conclusion can be made from this comparison: the least squares algorithm and the general type analytical algorithm produce close results. Some deviation in the retrievals for error-free cases may be explained by a possible effect of the weighting function implicitly embedded into the least-squares algorithm.

Table 6. Comparison of the Retrievals for the Least-squares and General Analytical Algorithms

Average Value of Random Errors in Reflectance, %	Bio-Optical Parameter	Correlation Coefficient	Average Relative Discrepancy, r1, %
0.0	*C*	0.992	5.6
	a	0.994	2.5
	S	0.999	2.6
5.0	*C*	0.918	32.0
	a	0.957	17.8
	S	0.944	10.9

3.4.4 Comparison of the Matrix-Inversion Algorithm With an Empirical Algorithm

A comparison of the matrix-inversion algorithm with an empirical algorithm is not straightforward for modeled reflectance data sets. Even for undisturbed reflectance the empirical algorithm produces retrievals with inherent errors because of the inconsistency of reflectance models with empirical algorithms. Moreover, the empirical algorithms may totally fail for Case 2 water reflectance.

Retrieval errors of an empirical algorithm caused by errors in water-leaving radiance can be easily estimated. For example, for the empirical algorithm given by Equation 1, the SPM relative error is determined by the expression:

$$\frac{\Delta S}{S} = B\left(\frac{\Delta L_1}{L_1} - \frac{\Delta L_2}{L_2}\right) \tag{25}$$

where L_i, i=1,2 is water-leaving radiance at i-th wavelength. In the case of spectrally uncorrelated random errors in the water-leaving radiance, the relative errors of the water-leaving radiance should be summed, i.e., $\Delta S/S = 2B\,\Delta L/L$. However, this estimate gives only the algorithm precision, i.e., the standard deviation of an estimated value of SPM concentration. The difference between the mean estimated value of SPM and its true value characterizing the algorithm accuracy cannot be evaluated in such a way.

Retrieval uncertainties of the empirical algorithm (Equation 1) were evaluated using simulated reflectance spectra. Reflectance spectra were simulated for both Case 1 water and Case 2 water. The Case 1 water reflectance spectra were generated using a seawater IOP model taken from Morel (1988).

According to this model the particulate backscattering coefficient is given by Equation 12, and the total absorption coefficient is given by the following expression:

$$a=(a_w+0.06AC^{0.65})(1+g\exp(-0.014(\lambda-440))) \quad (26)$$

where A is the wavelength-dependent coefficient (Bricaud *et al*., 1981), C is the chlorophyll concentration in mg/m^3, and g=0.2 is the fraction of DOM absorption at 440 nm. The chlorophyll concentration is the only input parameter of the reflectance model. The reflectance data set is generated assuming the lognormal distribution of the chlorophyll concentration with the mean equal to 0.3 mg/m^3 and the standard deviation equal to 1.0 mg/m^3.

The Case 2 water reflectance spectra were generated as described in paragraph 3.4.2.1. Some results for the empirical algorithm are given in Table 7 for Case 1 and Case 2 waters. Simulated reflectance spectra were not disturbed by errors. The correlation coefficients between initial and retrieved quantities are also given in the table to characterize the retrievals further.

Table 7. Errors in Retrieved SPM Concentration

	Relative Error for Case 1 Water, r_1 %	Correlation Coefficient	Relative Error for Case 2 Water, r_1 %	Correlation Coefficient
Empirical algorithm	14.4	0.990	79.6	-0.565
Matrix-inversion algorithm	6.4	0.992	10.8	0.954

Table 7 shows that the retrieval uncertainty of the empirical algorithm is quite acceptable for Case 1 waters. At the same time the empirical algorithm totally fails for Case 2 waters, producing even negative value of the correlation coefficient. To roughly compare the empirical algorithm with the matrix-inversion algorithm, results for the matrix-inversion algorithm are also given in Table 7 for 5 percent spectrally uncorrelated random error in water-leaving radiance.

3.4.5 Sensitivity Study Conclusions

The sensitivity study was conducted for simulated reflectance data sets modeling both Case 1 and Case 2 waters. Simulated reflectance spectra were perturbed with two types of errors: spectrally uncorrelated random errors modeling sensor radiometric noise; and spectrally correlated errors modeling sensor calibration and/or atmospheric correction errors. The algorithm was applied for the reflectance spectra simulated at five VIIRS visible bands: 413; 443; 488; 556; and 672 nm. (SeaWiFS visible bands 412, 443, 490, 510, 555, and 670 nm were also used for comparison of results). The chlorophyll-specific absorption coefficient was taken as being either dependent on or independent of chlorophyll concentration. In all cases the reproduction of the simulated reflectance spectra by retrieved reflectance spectra was quite good. A spectrally averaged deviation between the simulated and retrieved reflectance spectra was usually a few percent, reaching 10 percent in rare cases.

The sensitivity study showed that the spectrally uncorrelated random errors in reflectance spectra are significantly amplified in the retrieval errors. It was found that retrieved chlorophyll

concentration is most sensitive to spectrally uncorrelated errors in reflectance spectra. The ±5 percent random error in reflectance spectra typically results in about 30 percent error in chlorophyll concentration, 20 percent error in the DOM absorption coefficient, and 10 percent error in SPM concentration for the chlorophyll-specific absorption coefficient being independent of chlorophyll concentration. In the case of the chlorophyll-specific absorption coefficient dependent on chlorophyll concentration, the error in chlorophyll concentration doubles while the error in the DOM absorption coefficient and SPM concentration increases only weakly.

The spectrally correlated errors in reflectance spectra are not amplified significantly in the retrieval errors. It was found that retrieved SPM concentration is most sensitive to these types of errors modeling imperfect atmospheric correction and/or sensor calibration errors. The 20 percent error in the red band reflectance results in approximately a 15 percent error in chlorophyll concentration, a 5 percent error in the DOM absorption coefficient, and a 25-30 percent error in SPM concentration for the Angstrom exponent setting to zero and the chlorophyll-specific absorption coefficient independent of chlorophyll concentration. Setting the Angstrom exponent to unity, i.e., increasing the error value in the short-wavelength range, mainly enhances the error in the DOM absorption coefficient. The errors in chlorophyll and SPM retrievals increase weakly. In the case of the chlorophyll-specific absorption coefficient dependent on chlorophyll concentration, the same thing takes place. The error in chlorophyll doubles while the error in the DOM absorption coefficient and SPM concentration increases only weakly.

In all cases, retrieval accuracy is somewhat better, provided the backscatter wavelength ratio exponent, n, and the DOM absorption spectral slope, k, is known.
For Case 2 waters, the effect of uncertainty in the pure seawater absorption coefficient on the retrievals is small because of a small contribution of water absorption to the total absorption. Possible relative errors in the retrieved bio-optical parameters due to the pure seawater absorption coefficient uncertainty are about a few percent. For Case 1 waters the effect of uncertainty in the pure seawater absorption coefficient on the retrievals is considerable. Relative errors in the retrieved SPM concentration parameters due to the pure seawater absorption coefficient uncertainty are about 15 percent.

Overall evaluation of the algorithm can be formulated as follows. The algorithm is little sensitive to radiometric noise in the remote sensing reflectance. Meanwhile, the algorithm is sensitive to spectrally correlated perturbations in the remote sensing reflectance caused by atmospheric correction and/or sensor calibration error. Vicarious calibration of the sensor and algorithms is crucial for the mass loading algorithm.

Magnitudes of the intrinsic algorithm errors were adopted on a basis of above simulations and following considerations. The random algorithm error should include an uncertainty of the mass loading retrievals, which is due to the natural variability of optically active constituents not accounted for by the algorithm. The natural variability may include the particle size distribution variability, pigment species variability, and bi-directional effects of the seawater reflectance. Other types of the natural variability are accounted for by the algorithm. Finally, the natural variability affects the coefficient, which converts the mass loading backscattering coefficient to the mass loading. So far, information on the conversion coefficient variability is very limited because of the difficulty in measuring the seawater backscattering coefficient. The uncertainty of

the measurements of the backscattering coefficient is about 15-20% (Maffione and Dana, 1997). The algorithm precision due to the natural variability was accepted to be equal to 15%. This best estimate of the algorithm precision is consistent with the backscattering coefficient measurement uncertainty. In fact, this number is tentative and will be refined when the new data becomes available.

Unfortunately, there is no comprehensive database of *in situ* measured values of mass loading and reflectances like the SeaBAM database for chlorophyll (O'Reilly *et al*., 1998). Therefore, the bio-optical algorithm systematic error was estimated using the results of the sensitivity study. Estimates of the bio-optical algorithm error were done by simulations of the mass loading retrievals from the reflectance model with uncertainties introduced in IOPs. The effect of uncertainty in the pure seawater absorption coefficient on the retrievals is the most important because of the large difference between the "new" values (Pope and Fry, 1997) and the "old" values of the pure seawater absorption coefficient (Smith and Baker, 1981). For Case 2 turbid waters, the effect of uncertainty of the pure seawater absorption coefficient on the retrievals is relatively small because of the small contribution of water absorption to the total absorption. The error in the SPM concentration is only a few percent. For Case 1 waters, the "new" values of the pure seawater absorption coefficient dramatically change the spectral reflectance because of the large contribution of pure seawater absorption to the total absorption of seawater (Morel, 1996). The relative error of SPM retrievals is about 15 percent. Therefore, the algorithm systematic error was accepted to be equal to 15% for SPM < 1.0 mg/l and 10% for SPM > 1.0 mg/l. These estimates of the algorithm random and systematic errors were used in simulations described below.

A very limited dataset of *in situ* measured mass loading (Clark *et al*., 1980) was used to estimate the uncertainty of mass loading retrieved by the empirical algorithm. The mass loading algorithm switches to the empirical algorithm in exception cases when the physical retrieval algorithm fails to retrieve the mass loading EDR. According to Clark *et al*., 1980, the standard error of the mass loading estimate by the band ratio regression is about 0.20 mg/l or 25%.

3.4.6 Sensor Specification and Predicted Performance

Final simulations were done for radiometric noise corresponding to sensor specification and predicted performance. A general scheme of the simulations is shown in Figure 12. For a given SPM concentration, the remote sensing reflectance was calculated using reflectance models for Case 1 and Case 2 waters. For Case 1 waters, the well-known reflectance model suggested by Morel (1988) was used. SPM concentration was directly related to chlorophyll concentration using Equation 23. For Case 2 waters, a simplified reflectance model based on empirical regressions by Tassan (1994) was used (Vasilkov, 1997). The empirical regressions related both the SPM concentration and DOM absorption coefficient to chlorophyll concentration. Therefore, the chlorophyll concentration is the only input parameter of the model. According to this model, suspended particulate matter (SPM) concentration is higher for a given chlorophyll concentration than for the Case 1 reflectance model. The model can be referred to as a sediment-rich reflectance model.

TOA radiances were calculated using both the adapted two-layer model after Gordon and Wang (1994) and radiative transfer code by Liu and Rupert (1996). A maritime aerosol model with

humidity of 80% was used in simulations of the TOA radiances. This aerosol model having humidity of 80% was not included in candidate models of the atmospheric correction algorithm. Most simulations were done for a baseline visibility range of 23 km corresponding to aerosol optical thickness of 0.15 at wavelength of 550 nm. Simulation geometries correspond to the 13:30 satellite orbit.

The TOA radiances were perturbed by gaussian radiometric noise representing both sensor specification and predicted performance *[V-3]*. A spectrally correlated calibration error of 0.5% was added to the TOA radiances. The value of the calibration error is believed to be reasonable for the post-launch vicarious calibration of the sensor and algorithms (Gordon, 1997). The TOA radiances were also perturbed by a whitecap reflectance error corresponding to an uncertainty in wind speed of 1 m/s at a nominal value of wind speed of 6 m/s. Sensor polarization sensitivity was assumed to be equal to 3% in all visible and NIR bands with an uncertainty of 0.5%.

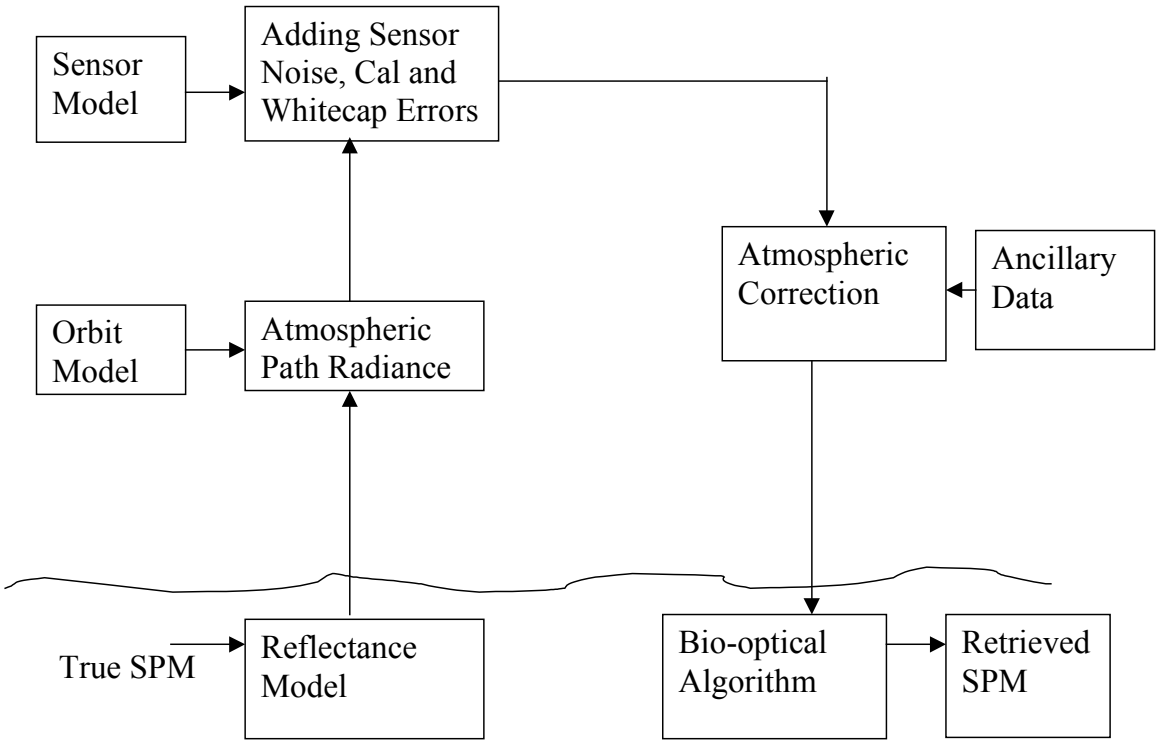

Figure 12. Shows a general scheme of simulations carried out to estimate the Mass Loading accuracy and precision for sensor specification and predicted performance.

Atmospheric correction was applied to the perturbed TOA radiances to retrieve remote sensing reflectances. The atmospheric correction algorithm (Gordon and Wang, 1994) was modified to include sensor polarization sensitivity correction. More details can be found in the Atmospheric Correction over the Ocean ATBD (SRBS Document # Y2411, version 3, 2000). SPM concentrations were retrieved from the remote sensing. The retrieved SPM concentrations were compared to the true SPM concentrations and SPM precision and accuracy were calculated. The SPM precision depends on both the solar zenith angle (SZA) and viewing geometry. Therefore,

the SPM precision was calculated at nadir and edge of swath (EOS) by averaging over SZA of the satellite orbit. The SPM accuracy appeared to be almost independent of viewing geometry.

The precision for the moderate resolution product is shown in Figure 13 as a function of true SPM concentrations. The Case 1 water reflectance model was used for the moderate resolution product, which will be retrieved for regions at distances more than 370 km off a coastline. Pixel aggregation reducing the radiometric noise effects in all bands was made to the cell size of 2.6 km. The Mass Loading precision threshold and objective are also shown in the figure along with A-Specification. It is seen from Figure 13 that sensor predicted performance is significantly better than the sensor specification performance.

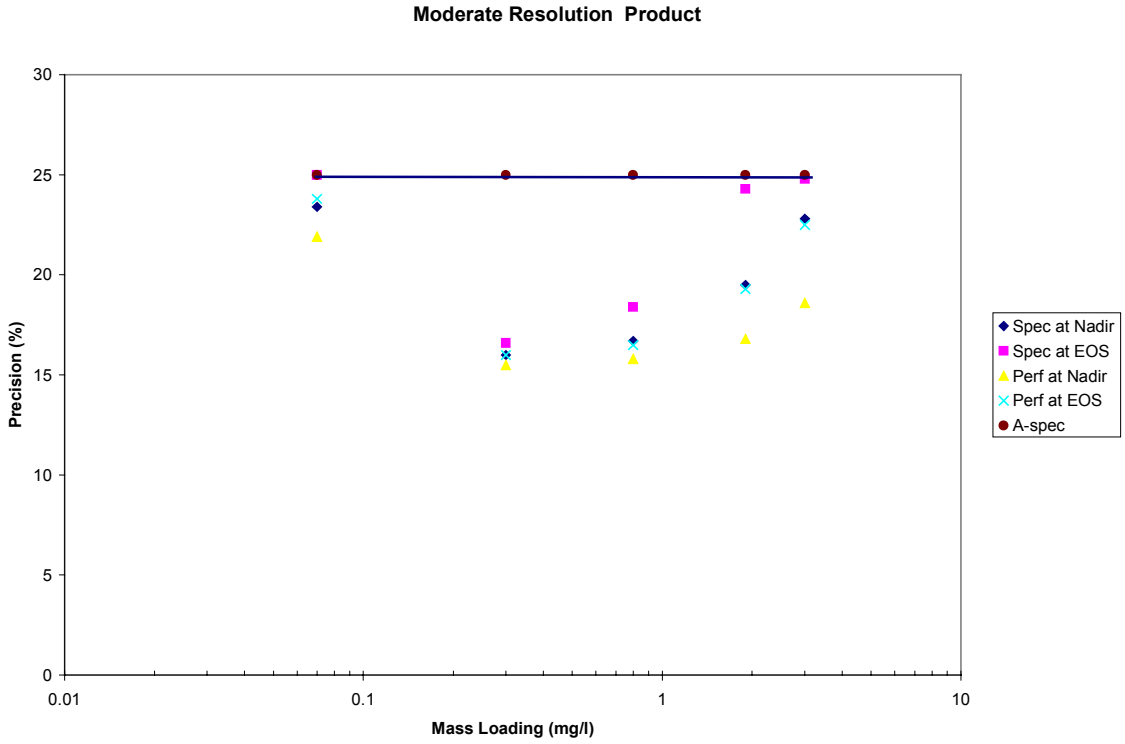

Figure 13. Shows Mass Loading precision as a function of Mass Loading values for radiometric noise of sensor specification and predicted performance. The Mass Loading precision is shown at nadir and edge of swath (EOS).

The Mass Loading accuracy for the moderate resolution product is shown in Figure 14. The Mass Loading accuracy threshold and objective are also shown in the figure along with A-Specification. It is seen from Figure 14 that the sensor predicted performance is quite close to the sensor specification performance.

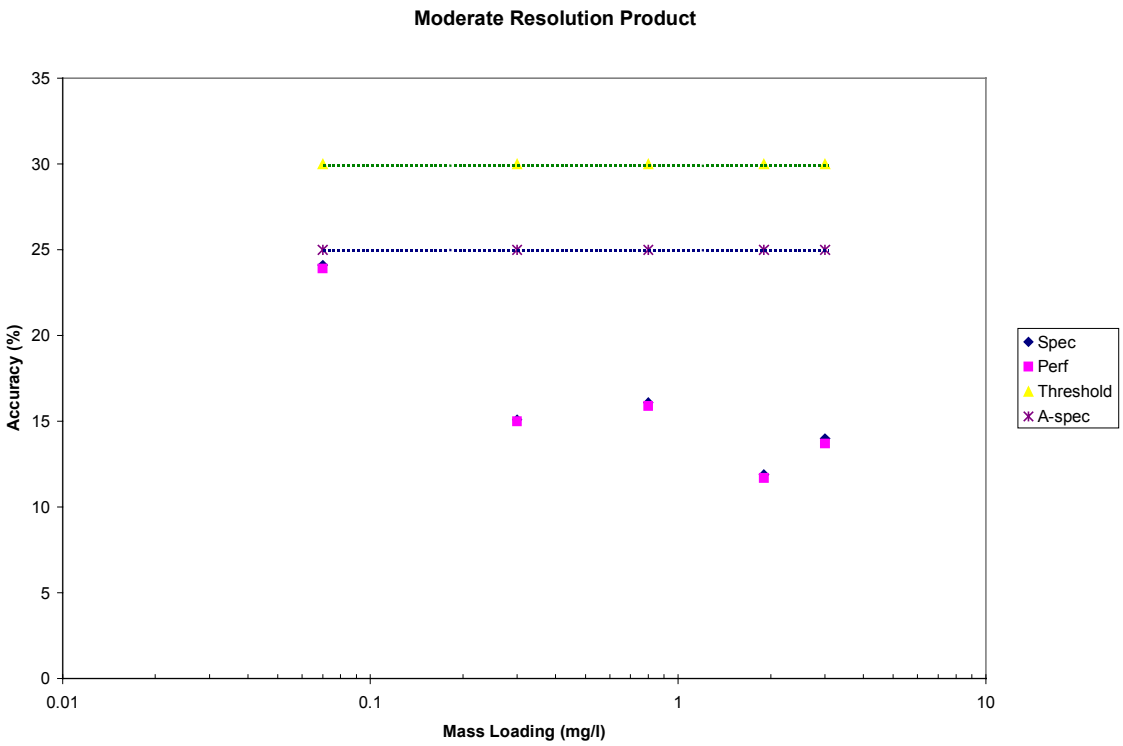

Figure 14. Shows Mass Loading accuracy as a function of Mass Loading values for the moderate resolution product.

The sediment-rich reflectance model was used for the fine resolution product, which will be retrieved for regions within 370 km of a coastline. No pixel aggregation was made except for the NIR bands supporting the atmospheric correction algorithm. The mass loading uncertainty for the fine resolution product is shown in Figure 15 as a function of true mass loading values. The mass loading uncertainty threshold is also shown in the figure along with A-Specification. It is seen from Figure 15 that sensor predicted performance is close to the sensor specification performance.

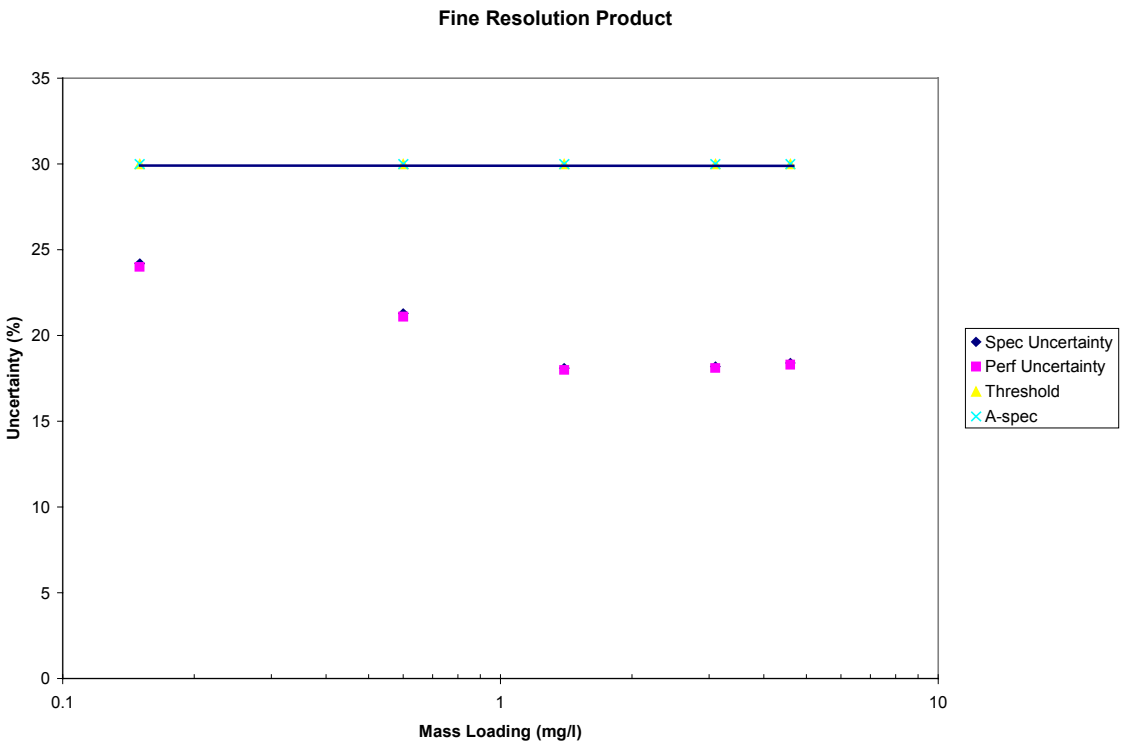

Figure 15. Shows Mass Loading uncertainty as a function of Mass Loading values for the fine resolution product.

3.5 PRACTICAL CONSIDERATIONS

3.5.1 Numerical Computation Considerations

The algorithm based on the linear least-squares technique is computationally fast. For the chlorophyll-specific absorption coefficient independent of chlorophyll concentration, the inversion of the reflectance model for one pixel takes about 10^{-3} second of run-time on Silicon Graphics Origin 2000 with 250 MHz CPU.

3.5.2 Programming and Procedural Considerations

The algorithm is based on the linear least-squares technique. To solve the linear least-squares problem, the singular value decomposition (SVD) method is used. At present, a computer program implementing the algorithm uses a subroutine (SVDCMP) of Numerical Recipes, which constructs the SVD of any matrix (Press *et al*., 1992).

3.5.3 Configuration of Retrievals

A configuration file is used to establish the numerical values of adjustable parameters used within the retrieval, e.g., a parameter indicating whether the chlorophyll-specific coefficient depends on chlorophyll concentration, and a corresponding threshold establishing whether an iteration on chlorophyll concentration may be terminated. This avoids specific values in the

software and allows adjustment of the algorithm to specific ocean areas such as coastal waters. The contents of the configuration file are shown in Table 8. The values shown correspond to the preliminary settings.

Table 8. Contents of the Configuration File

Parameter	Value
Parameter JC, defining whether the chlorophyll-specific absorption coefficient depends on chlorophyll concentration	1 if yes 0 if no
Iteration convergence parameter for the case JC=1	0.1
Maximum number of iterations for the case JC=1	10
Minimum value of the DOM absorption spectral slope, k	0.014
Maximum value of the DOM absorption spectral slope, k	0.024
The DOM absorption spectral slope increments, Δk	0.001
Minimum value of the SPM backscatter wavelength ratio exponent, n	0.0
Maximum value of the SPM backscatter wavelength ratio exponent, n	2.0
The SPM backscatter wavelength ratio exponent increments, Δk	0.2
Parameter showing whether the 672 nm band should be discarded in the inversion (e.g., while processing clear water pixels with in-band radiance close to zero)	1 if yes 0 if no

3.5.4 Quality Assessment and Diagnostics

A number of parameters and indicators will be reported in the Mass Loading Product as retrieval diagnostics. Included among these are parameters of the configuration file, average accuracy of fitting the spectral water-leaving radiances with model radiances, and statistical information regarding the processing.

3.5.5 Exception Handling

A mass loading retrieval is performed only if the atmospheric correction algorithm provides positive values of water-leaving radiances in all VIIRS visible bands. If the algorithm fails in providing positive values of all retrievals, the SPM backscattering coefficient, the DOM absorption coefficient, and chlorophyll concentration, mass loading output will be set to –1.

3.6 ALGORITHM VALIDATION

Validation of the algorithm will rely on *in situ* measurements of spectral water-leaving radiance, the SPM backscattering coefficient, and SPM concentration.

4.0 ASSUMPTIONS AND LIMITATIONS

4.1 ASSUMPTIONS

The following assumptions are made with respect to the mass loading retrievals described in this document:

- Water-leaving radiances at VIIRS visible band wavelengths are available from an atmospheric correction algorithm.
- Water reflectance is described as a function of the ratio of the total backscattering coefficient to the sum of the total absorption coefficient and the total backscattering coefficient.
- Parameters describing the spectral backscatter of SPM and the spectral absorption of DOM can be adjusted when inverting the reflectance model.
- Mass loading is proportional to the SPM backscattering coefficient, the coefficient of proportionality being regionally specific.

4.2 LIMITATIONS

The following limitations apply to the mass loading retrieval described in this document:

- Retrievals will not be performed over a pixel for which atmospheric correction fails, resulting in zero or negative water-leaving radiance in any VIIRS visible band.
- Retrievals will not be performed over a pixel for which least-squares minimization results in a nonpositive solution to the backscattering coefficient for the entire ranges of all parameters to be adjusted when inverting the reflectance model.

5.0 REFERENCES

Aas, E. (1987). Two-stream irradiance model for deep waters. Applied Optics, Vol. 26, pp. 2095-2101.

Althuis, I.J.A., J. Vogelzang, M.R. Wernand, S.J. Shimwell, W.W.C. Gieskes, R.E. Warnock, J. Kromkamp, R. Wouts, and W. Zevenboom (1996a). On the colour of case 2 waters: particulate matter North Sea, Part I: Results and conclusions. Netherlands Remote Sensing Board Report 95-21B, 163 p.

Althuis, I.J.A., J. Vogelzang, M.R. Wernand, S.J. Shimwell, W.W.C. Gieskes, R.E. Warnock, J. Kromkamp, R. Wouts, and W. Zevenboom (1996b). On the colour of case 2 waters: particulate matter North Sea, Part II: Instruments, methods and database. Netherlands Remote Sensing Board Report 95-21B, 73 p.

Antoine D., J.-M. Andre, and A. Morel (1996). Oceanic primary production. 2. Estimation at global scale from satellite (CZCS) chlorophyll. *Glob. Biochem. Cycles*, Vol. 10, pp. 57-69.

Bricaud, A., A. Morel, and L. Prieur (1981). Absorption by dissolved organic matter of the sea (yellow substance) in the UV and visible domains. *Limnol. Oceanogr.*, Vol. 26, No. 1, pp. 43-53.

Bricaud, A., M. Babin, A. Morel, and H. Claustre (1995). Variability in the chlorophyll-specific absorption coefficients of natural phytoplankton: Analysis and parameterization. *J. Geophys. Res.*, Vol. 100, No. C7, pp. 13,321-13,332.

Burenkov, V.I., A.P. Vasilkov, and L.A. Stephantsev (1995). Retrieval of spectral inherent optical properties of sea water from the spectral reflectance. *Oceanology*, Vol. 25, No. 1, pp. 49-54.

Campbell, J.W. (1995). The lognormal distribution as a model for bio-optical variability in the sea. *J. Geophys. Res.*, Vol. 100, No. C7, pp. 13,237-13,254.

Carder K.L., and R.G. Steward (1985). A remote-sensing reflectance model of a red tide dinoflagellate off West Florida. *Limnology and Oceanography*, Vol. 30, pp. 286-298.

Carder, K.L., S.K. Hawes, K.A. Baker, R.C. Smith, R.G. Steward, and B.G. Mitchell (1991). Reflectance model for quantifying chlorophyll a in the presence of productivity degradation products. *J. Geophys. Res.*, Vol. 96, pp. 20,559-20,611.

Clark, D.K., E.T. Baker, and A.E. Strong (1980). Upwelled spectral radiance distribution in relation to particulate matter in sea water. *Boundary-Layer Meteorology*, Vol. 18, No. 3, pp. 287-298.

Doerffer, R., and J. Fisher (1994). Concentrations of chlorophyll, suspended matter, and gelbstoff in case II waters derived from satellite coastal zone color scanner data with inverse modelling methods. *J. Geophys. Res.*, Vol. 99, No. C4, pp. 7,457-7,466.

Dubovik, O.V., S.L. Oshchepkov, and T.V. Lapyonok (1994). Iteration-regularization method of solution of nonlinear inverse problems and its application to interpretation of the spectra of brightness coefficient of a layer of water. *Physics of Atmosphere and Ocean,* Vol. 30, pp. 103-110.

Garver, S.A., and D.A. Siegel (1997). Inherent optical property inversion of ocean color spectra and its biogeochemical interpretation: 1. Time series from the Sargasso Sea. *J. Geophys. Res*., Vol. 102, pp. 18,607-18,625.

Golubitskiy, B.M., and I.M. Levin (1980). Transmittance and reflectance of layer of highly anisotropic scattering medium. Izvestiya USSR Academy of Sciences. *Atmospheric and Oceanic Physics*, Vol. 16, pp. 926-931.

Gordon, H.R. (1973). Simple calculation of the diffuse reflectance of the ocean. *Applied Optics,* 12, 2803-2804.

Gordon, H.R., D.K. Clark, J.W. Brown, O.B. Brown, R.H. Evans, and W.W. Broenkow (1983). Phytoplankton pigment concentrations in the Middle Atlantic Bight: Comparison of ship determinations and CZCS estimates. *Appl. Opt*., Vol. 22, No. 1, pp.20-36.

Gordon, H.R. and A. Morel (1983). Remote assessment of ocean color for interpretation of satellite visible imagery. A review. N.Y. Springer, 114 pp.

Gordon, H.R., O.B. Brown, R.H. Evans, J.W. Brown, R.C. Smith, K.S. Baker, and D.K. Clark (1988). A semianalytic radiance model of ocean color. *J. Geophys. Res*., Vol. 93, pp. 10,909-10,924, 1988.

Gordon, H.R. (1989). Dependence of the diffuse reflectance of natural waters on the sun angle. *Limnology and Oceanography*, Vol. 34, pp. 1484-1489.

Gordon, H.R., and M. Wang (1994). Retrieval of water-leaving radiance and aerosol optical thickness over the oceans with SeaWiFS: a preliminary algorithm. *Applied Optics*, 33, 443-450.

Gordon, H.R. (1997). In-orbit calibration strategy for ocean color sensors. *Remote Sens. Environ*., Vol. 63, 265-278.

Hoge, F.E., and P.E. Lyon (1996). Satellite retrieval of inherent optical properties by linear matrix inversion of oceanic radiance models: An analysis of model and radiance measurement errors. *J. Geophys. Res.*, Vol. 101, No. C7, pp. 16,631-16,648.

Hoge, F.E., C.W. Wright, P.E. Lyon, R.N. Swift, and J.K. Yungel (1999). Satellite retrieval of inherent optical properties by inversion of oceanic radiance models: A preliminary algorithm. *Appl. Opt.*, Vol. 38, No. 3, pp. 495-504.

Hoogenboom, H.J., A.G. Dekker, and J.F. de Haan (1997). Inversion: interpretation of reflectance spectra for water quality assessment. Report of Institute for Environmental Studies. Amsterdam, 83 pp.

Hultrin, V.I., and G.W. Kattawar (1993). Self-consistent solutions to the equation of transfer with elastic and inelastic scattering in oceanic optics: I. Model. *Applied Optics*, Vol. 32, pp. 5356-5367.

Hoogenboom, H.J., A.G. Dekker, and J.F. de Haan (1997). Inversion: interpretation of reflectance spectra for water quality assessment. Report of Institute for Environmental Studies. Amsterdam, 83 pp.

Hucks, J. 1998, RSTX Internal Memorandum Y1629.

Hultrin, V.I. (1997). Monte-Carlo modeling of light field parameters in ocean with Petzold laws of scattering. Proceedings of the 4th International Conference on Remote Sensing for Marine and Coastal Environments. Orlando, Florida, 17-19 March 1997, Vol. I, pp. 502-508.

Liu, Q. and E. Rupert (1996). A radiative transfer model: matrix operator method. *Appl. Opt*., Vol. 35, 4229-4237.

Lee, Z., K.L. Carder, T.G. Peacock, C.O. Davis, and J.L. Mueller (1996), Method to derive ocean absorption coefficients from remote-sensing reflectance. *Appl. Opt*., Vol. 35, No. 3, pp. 453-462.

Maffione R.A. and D.R. Dana (1997). Instruments and methods for measuring the backward-scattering coefficient of ocean waters. *Appl. Opt*., Vol. 36, 6057-6067.

Miller S. (1998) Raytheon Internal Memorandum 98VIIRSL00026.

Morel, A. (1988). Optical Modelling of the Upper Ocean in Relation to Its Biogenous Matter Content (Case 1 Waters). *J. Geophys. Res*., Vol. 93, pp. 10749-10768.

Morel, A. (1996). Optical properties of oceanic Case 1 waters, revisited. *Ocean Optics XIII*, Proceedings SPIE. Vol. 1963, pp. 108-113.

Ouillon, S.,P. Forget, J.M. Froidefond, and J.J. Naudin (1995). Estimating suspended matter concentrations from SPOT data and from field measurements in the Rhone river plume. Proceedings of the 3rd Conference on Remote Sensing for Marine and Coastal Environments. Seattle, USA, 18-20 September 1995, Vol. 2, pp. 200-209.

Pope, R.M. and E.S. Fry (1997). Absorption spectrum (380-700 nm) of pure water. II. Integrating cavity measurements. *Applied Optics*, Vol. 36, pp. 8710-8723.

Press, W.H., S.A. Teukolsky, W.T. Vetterling, and B.P. Flannery (1992). Numerical Recipes in FORTRAN: The art of scientific computing. 2nd ed., Cambridge University Press, 963 pp.

Roesler, C.S. and M.J. Perry (1995). In situ phytoplankton absorption, fluorescence emission, and particulate backscattering spectra determined from reflectance. *Journal of Geophysical Research*, Vol. 102, pp. 13,279-13,294.

Sathyendranath, S., L. Prieur, and A. Morel (1989). A three-component model of ocean colour and its application to remote sensing of phytoplankton pigments in coastal waters. *Int. J. Remote Sensing*, Vol. 10, pp. 1373-1394.

Smith, R.C., and K.S. Baker (1981). Optical properties of the clearest natural waters. (200-800 nm). *Appl. Opt*., Vol. 20, No. 2, pp. 177-183.

Sogandares, F.M., and E.S. Fry (1997). Absorption spectrum (340-700 nm) of pure water. I. Photothermal measurements. *Applied Optics*, Vol. 36, pp. 8710-8723.

Sugihara, S., M. Kishino, and N. Okami (1985). Estimation of water quality parameters from irradiance reflectance using optical models. *J. Oceanog. Soc. Japan*, Vol. 41, pp. 399-406.

Tassan, S. (1994). Local algorithms using SeaWiFS data for the retrieval of phytoplankton pigments, suspended sediment, and yellow substance in coastal waters. *Appl. Opt.,* Vol. 33, 2369-2378.

Vasilkov, A.P., and L.A. Stephantsev (1987). Effect of solar elevation in remote measurements on the spectral composition of radiation exiting from the ocean. *Oceanology*, Vol. 27, No. 2, p. 163.

Vasilkov, A.P., and B.F. Kelbalikhanov (1991). Passive optical remote sensing of the ocean. USSR Academy of Sciencies, Syktyvkar, 107p., (in Russian).

Vasilkov, A.P, I.V. Geogdgaev, T.V. Kondranin, and N.A. Krotkov (1992). On accuracy of retrieval of sea water constituents concentrations from water-leaving radiance model. In *Problems of Hydrophysics and Geospace Physics*, MIPT, pp. 111-122, (in Russian).

Vasilkov, A.P. (1997). A retrieval of coastal water constituent concentrations by least-square inversion of a radiance model. Proceedings of the 4th International Conference on Remote Sensing for Marine and Coastal Environments. Orlando, Florida, 17-19 March 1997, Vol. II, pp. 107-116.

Vermote, E.F., D. Tanré, J.L. Deuzé, M. Herman, and J.J. Morcrette (1997). Second simulation of the satellite signal in the solar spectrum, 6S: An overview. *IEEE Trans. Geosci. Remote Sensing*, Vol. 35, p. 675.

Zaneveld, J.R.V. (1982). Remotely sensed reflectance and its dependence on vertical structure: a theoretical derivation. *Applied Optics*,.Vol. 21, pp. 4146-4150.

Zaneveld, J.R.V. (1995). A theoretical derivation of the dependence of the remotely sensed reflectance of the ocean on the inherent optical properties. *Journal of Geophysical Research*, Vol. 102, pp. 13,135-13,142.